PHENIX Beam Use Proposal for RHIC Run-12 and Run-13

The PHENIX Collaboration

June 1, 2011

1 Executive summary

We present the beam use proposal for Run-12 and Run-13, based upon the physics priorities of the PHENIX Collaboration, and laboratory guidance of 26 to 30 weeks in Run-12 and 26 weeks in Run-13. The list in this summary is priority-ordered. However, our preferred running order is different, as described below.

26 cryo-week proposal for Run-12:

1. 500 GeV p+p for 8 weeks
2. 200 GeV Au+Au for 7 weeks
3. 200 GeV p+p for 5 weeks
4. 193 GeV U+U for 1.5 weeks
5. 27 GeV Au+Au for 1 week

30 cryo-week proposal for Run-12:

1. 500 GeV p+p for 8 weeks
2. 200 GeV Au+Au for 7 weeks
3. 200 GeV p+p for 5 weeks
4. 193 GeV U+U for 1.5 weeks
5. 27 GeV Au+Au for 2 week
6. 62.4 GeV p+p for 1 week
7. 39 GeV p+p for 1 week

26 cryo-week proposal for Run-13:

1. 500 GeV p+p for 10 weeks
2. 200 GeV Cu+Au for 5 weeks
3. 200 GeV transverse p+p for 5 weeks
4. 193 GeV U+U for 5 weeks

Our twin highest priorities in the coming year will advance both the spin and heavy ion programs at RHIC. We aim to measure single-spin asymmetries of W bosons in the forward and backward direction in polarized 500 GeV p+p collisions, to determine light anti-quark polarizations. The other goal is to study separated charm and bottom quark propagation through the quark gluon plasma utilizing our new silicon vertex detectors. The latter requires full energy Au+Au running with maximum luminosity plus comparison running with 200 GeV p+p collisions.

Our next priority is to study U+U collisions, which are expected to access higher energy density in the tip-to-tip collision configuration and higher eccentricity in the side-to-side configuration. Both are of great interest, however our ability to control the geometry experimentally has yet to be demonstrated. Consequently, we request an exploratory

U+U run in Run-12, followed by a longer U+U run in Run-13 once analysis of the Run-12 data shows that collisions of different orientation can be selected.

Our fourth priority is continue the Au+Au energy scan. The PHENIX goals are to search for the onset of high p_T hadron suppression and the $\sqrt{s}$ where elliptic flow (v_2) reaches the saturated value observed at the higher RHIC energies and the LHC. Should Run-12 funding allow for 30 cryo weeks, we request p+p comparison running at 62.4 and 39 GeV. This will allow determination of R_{AA} instead of R_{cp} to help understand the intriguing new results on J/ψ suppression at 62.4 and 39 GeV from the Run-10.

Beginning in 2013, an exciting new priority for PHENIX will be to use asymmetric heavy ion collisions to study smaller systems with a well-controlled geometry. This will allow us to move path-length dependence studies of energy loss and J/ψ suppression from qualitative to quantitative.

In the following, we present highlights of recent PHENIX accomplishments to illustrate how we have made use of past RHIC conditions. We also present the current state of the experiment, our near term upgrade plans, and then discuss the physics that drives our proposed run plan. These latter points were, in large part, also described at length in the decadal plan developed and submitted by PHENIX on October 1, 2010. Because of that, portions of the following are reproduced from that document, updated where appropriate to reflect developments that have occurred since October.

2 Introduction

The PHENIX Collaboration proposes a scientific program of precision measurements to pursue key goals in the study of heavy ion collisions and the spin of the proton at RHIC. We aim to quantify the properties of the perfect QCD liquid, discover the conditions under which those properties are first manifested, address the puzzle of how the half integer spin of the nucleon is carried by its partonic constituents, and gain insight into the dynamical nature of and correlations among the partons in the nucleon.

The physics goals of the PHENIX Collaboration continue to evolve with increasing knowledge, higher luminosities, and improved detection capabilities, but a consistent theme is

the need for the highest possible integrated luminosities (and polarizations in the case of p+p running) to explore fully the range of fundamental phenomena in nucleus+nucleus, deuteron+nucleus and proton+proton collisions. The PHENIX detector was optimized for precision measurements of rare probes of partonic matter and polarized protons with particular focus on hard and electromagnetic probes. The experiment utilizes selective triggers, high rate capability, and multiple fast detector systems to track and identify particles. Over the years, our triggering, data acquisition, archiving, and data analysis have kept up with RHIC accelerator improvements. We applaud the C-AD developments of stochastic cooling, and request annual full energy Au+Au runs to utilize this key improvement in RHIC capabilities for physics production.

PHENIX has undertaken an ambitious upgrade program to further enhance and augment our capabilities. A major upgrade for triggering on high momentum muons from W decays has been commissioned during Run-11. The new silicon microvertex barrel detector (VTX) has been successfully installed, commissioned, and utilized. The VTX occupies the space vacated by the Hadron Blind Detector (HBD), which was removed following Run-10. In Run-12, the microvertex capabilities of PHENIX will be extended by the forward vertex detector (FVTX). We look forward to using these detectors and the increased luminosity afforded by stochastic cooling of heavy ion beams and electron lenses for proton beams. In spite of these undertakings, PHENIX continues to successfully provide timely data analysis using the RHIC Computing Facility (RCF) and computing resources at PHENIX collaborating institutions.

The period of 500 GeV p+p running during Run-11 presented PHENIX with significant challenges. The polarization of the 500 GeV p+p was, as anticipated near 50% and represented a significant improvement over the polarization achieved during Run-9; the integrated luminosity, however, fell rather short of expectations. The difficulty of obtaining consistently usable stores in the machine, regardless of the intensity, presented the VTX commissioning with its own challenges. The main effect is slowed progress toward the goals laid out in the RHIC Spin Research plans. We present in this Beam Use Proposal a plan for the next two years that takes this into account and also takes optimum advantage of the exciting PHENIX upgrades and anticipated RHIC luminosity increases.

The PHENIX Beam Use Proposal is guided by the carefully structured, ongoing program of upgrades. Our Run-12 request is optimized to take advantage of the muon trigger and silicon central barrel vertex detector (VTX) upgrades. The muon trigger will allow us to make significant progress on our measurement of W production and asymmetry at forward rapidity, and the VTX will provide a clear separation of c and b quark probes in

Au+Au collisions. The Muon Trigger upgrade will be completed with the construction and installation of the RPC-1 detector stations during the 2011 shutdown. The VTX assembly was finished and the detector was installed prior to the beginning of Run-11. A new Be beam pipe with small diameter was installed prior to Run-11. Construction of the forward vertex detector (FVTX) is well underway, and the FVTX will be completed for installation prior to Run-12.

3 Recent scientific accomplishments

Between mid-2010 and the present, PHENIX submitted sixteen new papers for publication. Those papers, and the entire PHENIX body of publications, have continued to accumulate citations at a steady rate, as shown in Figure 1. Collaborators have given more than 160 PHENIX talks, both invited and contributed, since the time of the last PAC meeting.

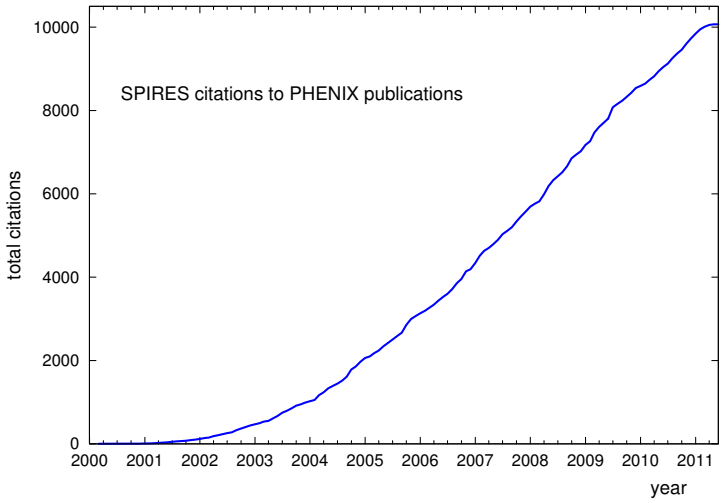

Figure 1: History of citations to PHENIX publications showing a steady accumulation over the last decade. The collaboration has more than 100 publications and more than 10,000 citations.

Among the papers recently submitted for publication are several results from the d+Au run taken in 2008. These results, on the path length dependence of J/ψ suppression and on dihadron correlations in d+Au with a variety of rapidity gaps between the hadrons

both shed light on the initial state for Au+Au collisions. Both measurements utilize our ability to classify the centrality of the d+Au collisions and point to large effects when gluonic matter becomes very dense.

J/ψ measurements over a wide kinematic range with high statistical precision [6] constrain the combination of nuclear shadowing and breakup in cold nuclear matter. In fact, calculations with the EPS09 nuclear parton distribution functions and a fixed break-up cross section in nuclear matter have difficulty reproducing the centrality dependence and the overall level of forward J/ψ suppression simultaneously. Comparison to a simple geometrical model of cold nuclear matter effects indicates that break-up based upon a linear or exponential density-weighted longitudinal thickness does not reproduce our data. The dependence of forward J/ψ yield is better approximated by a quadratic dependence. These data may be an early indication of effects of gluon saturation. However, before drawing a firm conclusion about this, other explanations involving initial state energy loss need further investigation.

In the second new result, back-to-back rapidity-separated hadron pair yields were measured in d+Au and p+p collisions [12]. Pairs were also detected with both hadrons at forward rapidity. Together these dihadrons provide hard scattering probes over a wide kinematic range. The yield of back-to-back hadron pairs in d+Au collisions with small impact parameters is observed to be suppressed by a factor of 10 relative to p+p. The kinematics of these pairs should probe partons at low x in the gold nucleus, where gluon densities rise sharply. The observed suppression appears to indicate large nuclear effects in the gluon structure of nucleons at small x. Again, there are caveats to the interpretation of dihadrons at relatively modest p_T values of 0.5–1.5 GeV/c, which may contain contributions from soft processes. However, this measurement also provides hints of interesting physics in regions of high gluon density.

3.1 Insights regarding particle flow in Au+Au

In Run-10, PHENIX continued the accumulation of substantial data sets on $\sqrt{s_{NN}} = 200$ GeV Au+Au collisions. These data sets allow study of a number of probes of the quark gluon plasma. While much of our physics focus is on hard probes, and analysis of the 2010 data is underway, a number of precision measurements of particle flow were completed over the past year.

A key new insight is the importance of fluctuation-driven odd harmonics of the flow field. These can be quantified by the third Fourier coefficient, v_3. PHENIX has recently measured flow coefficients v_2, v_3, and v_4 relative to event planes determined at large rapidity using our reaction plane detector, the muon piston calorimeter, and the beam-beam counters, located at rapidities of 1–2.8, 3.1–3.9, and 3.1–3.7, respectively [11]. We found that the event planes for v_2 and v_3 are uncorrelated, as expected for a triangular v_3 shape driven by event-by-event fluctuations in the participant nucleon density. The magnitudes of the Fourier coefficients were studied as a function of transverse momentum and collision centrality, and compared to hydrodynamic calculations from several authors, all employing initial state fluctuations.

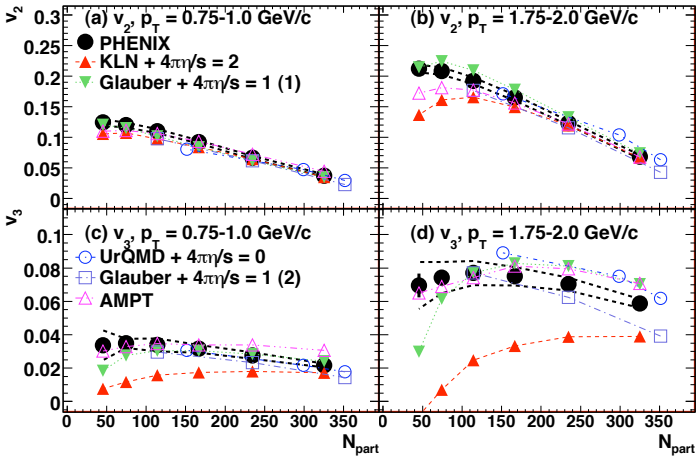

Figure 2: Comparison of v_2 and v_3 vs. N_{part} measurements in two ranges of p_T with theoretical predictions. The dark dashed lines around the data points indicate the size of the systematic uncertainty, and the symbols indicate the different predictions.

Figure 2 illustrates the new constraining power of the higher harmonics. It has been known for some time that the unknown initial state for hydrodynamics calculations drives a large uncertainty in the viscosity to entropy ratio (100%!), with v_2 unable to distinguish between color-glass-condensate and Glauber initial states. Indeed, one sees in the top two panels that v_2 is described equally well with hydrodynamics utilizing a color-glass-condensate initial state and viscosity to entropy ratio of $\eta/s = 2$ (red upward triangles labeled KLN) and a Glauber initial state with $\eta/s = 1$ (green downward triangles labeled Glauber). The bottom panels show that v_3 breaks the degeneracy, favoring the Glauber initial conditions with $\eta/s = 1$. This new constraint will allow us to significantly improve the precision of the extracted viscosity to entropy density ratio, which is one of the major goals of the RHIC program. The final answer, with error bar, requires joint work with theorists to constrain the parameters with data. It should be noted that the failure of the calculation utilizing the KLN formulation of color glass condensate initial state may be

due, at least in part, to details of how the initial state is implemented. This must also be investigated in order to set a well-understood error bar for η/s.

A second, very exciting new result, is first observation of direct photon flow. This is a measurement that only PHENIX can do; LHC experiments will have difficulty measuring direct photons in the range $1 < p_T < 3\,\mathrm{GeV}/c$. We have measured the v_2 of direct photons at midrapidity and $1 < p_T < 15\,\mathrm{GeV}/c$ in Au+Au collisions at $\sqrt{s_{NN}} = 200\,\mathrm{GeV}$. This was achieved by careful measurement of v_2 of inclusive photons and of π^0s in the PHENIX electromagnetic calorimeter. Flow of the decay photons is determined from the flow measurement of the neutral pions. Elliptic flow of the direct photons is then calculated as

$$v_2^{\gamma,\mathrm{dir}} = \frac{R_\gamma(p_T)v_2^{\gamma,inc} - v_2^{\gamma,\mathrm{bckg}}}{R_\gamma(p_T) - 1},$$

where $R_\gamma(p_T) = N^{\mathrm{inc}}(p_T)/N^{\mathrm{bckg}}(p_T)$ is the ratio of inclusive to hadron decay photons or "direct photon excess ratio". $N^{\mathrm{inc}} = N^{\mathrm{meas}} - N^{\mathrm{hadr}}$, i.e. the number of measured photons after subtraction of hadrons which survive the photon identification cuts. Values of $R_\gamma(p_T)$ above $5\,\mathrm{GeV}/c$ are taken from the real photon measurement with the PHENIX EMCal [14], and below that from the more accurate but $\mathrm{p_T}$-range limited internal conversion measurement of direct photons [7].

Figure 3 shows that for $p_T > 4\,\mathrm{GeV}/c$, the anisotropy of direct photons is consistent with zero, as expected for photons produced in initial hard scattering. However, for $p_T < 4\,\mathrm{GeV}/c$, a region dominated by thermal photons, we find a substantial direct photon v_2. Surprisingly, it is comparable to that of hadrons. Hydrodynamic model calculations for thermal photons in this kinematic region significantly underpredict the observed v_2, and the source of the flow is currently unknown. Flow of photons produced in the hadronic phase is already included in the hydrodynamic models, though pre-equilibrium flow, which is required to reproduce observed two particle Hanbury-Brown Twiss correlations, is not.

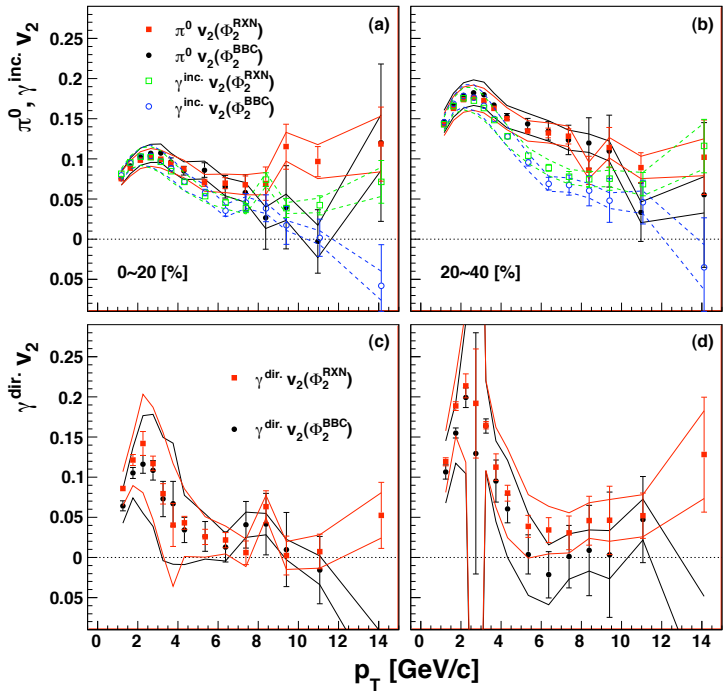

Figure 3: Centrality dependence of the π^0 and inclusive photon v_2 (a) 0–20%, (b) 20–40%. (c) direct photon v_2 for 0–20%, (d) same for 20–40% centrality.

3.2 Beam energy scan results

During Run-10, RHIC provided collisions of Au+Au at energies below the top energy of $\sqrt{s_{NN}} = 200\,\text{GeV}$ to enable a search for a critical point in the QCD phase diagram. PHENIX took significant data sets at $\sqrt{s_{NN}} = 62.4$, 39 and 7.7 GeV and has several new results based on that data. We have looked at the behavior of various Fourier coefficients describing the azimuthal momentum distribution as a function of collision energy. A compilation of our recent results for this observable can be seen in central events in Figure 4. The overall strength of the anisotropy falls as one looks at higher order coefficients, even while each of the coefficients rises with transverse momentum, but there seems to be very little energy dependence from 39 up to 200 GeV.

If one takes particular p_T selections of the v_2 shown in the leftmost panel of Figure 4 one can compare our new results with those of other experiments over a very wide range of collision energies. Figure 5 shows PHENIX results alongside results from significantly lower and significantly higher energy. From 39 GeV up to the LHC collision energy of

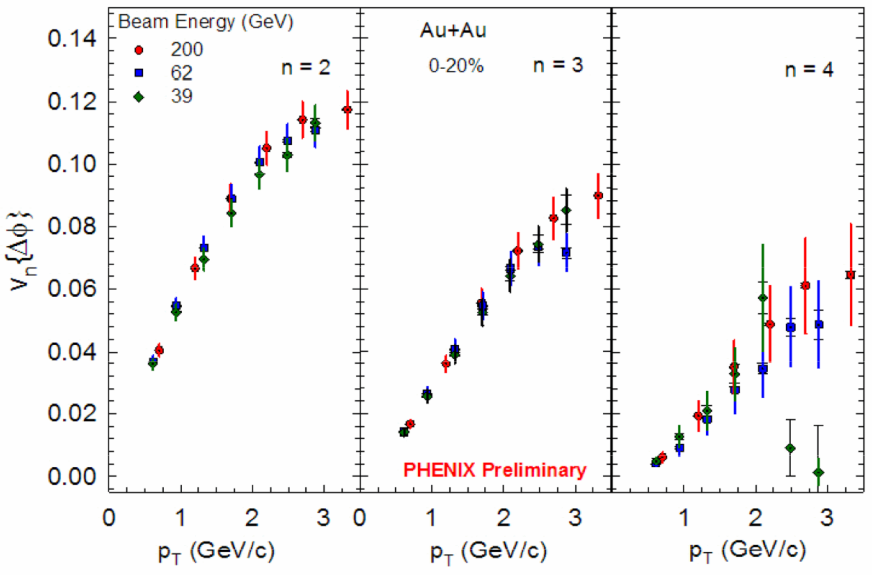

Figure 4: Comparison of higher order flow coefficients in Au+Au collisions at $\sqrt{s_{NN}} = 200$, 62.4 and 39 GeV.

2.76 TeV, one sees very little change in the strength of the elliptic flow reported in this way.

One expectation of the beam energy scan is that it will enable the RHIC experiments to identify the point in collision energy at which key observables supporting a partonic view of RHIC matter change their values. In particular, PHENIX has expressed an interest in seeing the collision energy at which participant quark scaling ceases to work well in describing the elliptic flow results. Figure 6 shows, for collisions at $\sqrt{s_{NN}} = 39$ GeV, the Fourier coefficient v_2 versus p_T on the left and v_2/n_q versus transverse kinetic energy, KE_T/n_q, on the right. Even at this rather low collision energy the constituent quark scaling appears to work quite well, The energy at which this scaling breaks down is clearly lower than this value of $\sqrt{s}$ and the collaboration is looking forward to continuing this analysis with collisions at even lower energy.

PHENIX has also looked at the behavior of rather hard probes at a function of the RHIC collision energy. Figure 7 shows one measure of the nuclear modification factor, R_{CP}, for $J/\psi \rightarrow \mu^+\mu^-$ in Au+Au collisions at $\sqrt{s_{NN}} = 200$, 62.4 and 39 GeV. Comparing the results at lower energies, one sees that they are consistent with the results from full energy RHIC collisions. The production of quarkonia is one of the most durable puzzles of high energy collision and these results add to the growing encyclopedia of data that will help

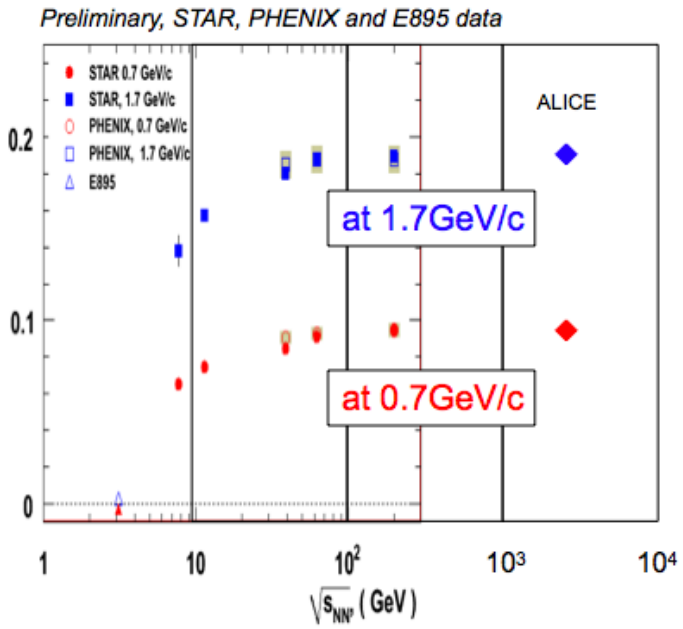

Figure 5: The second-order flow coefficient, v_2, in A+A collisions as a function of $\sqrt{s_{NN}}$, showing little change as $\sqrt{s_{NN}}$ rises from 39 GeV to 2.76 TeV.

resolve this mystery. It should be noted, however, that a more quantitative study of the $\sqrt{s}$ dependence of J/ψ suppression will require p+p reference data so that we may determine R_{AA} instead of relying upon the central to peripheral collision yield ratio. Ultimately, d+Au running at lower energy will also be required, in order to disentangle cold nuclear matter effects from suppression in quark gluon plasma. We anticipate requesting this in Run-14.

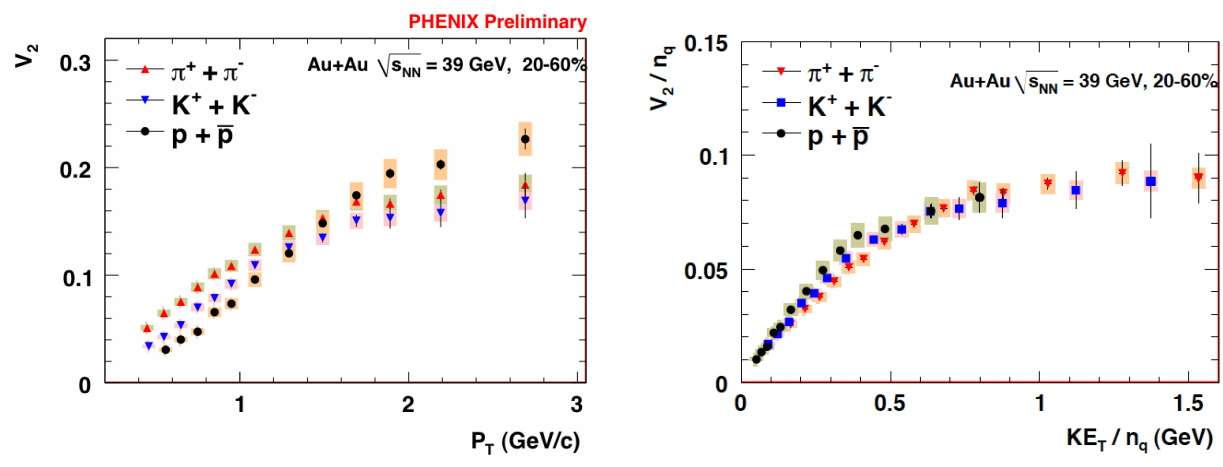

Figure 6: (left) Second-order flow coefficient for identified particles as a function of p_T. (right) v_2 divided by number of constituent quarks, n_q, as a function of the transverse kinetic energy KE_T, also divided by n_q.

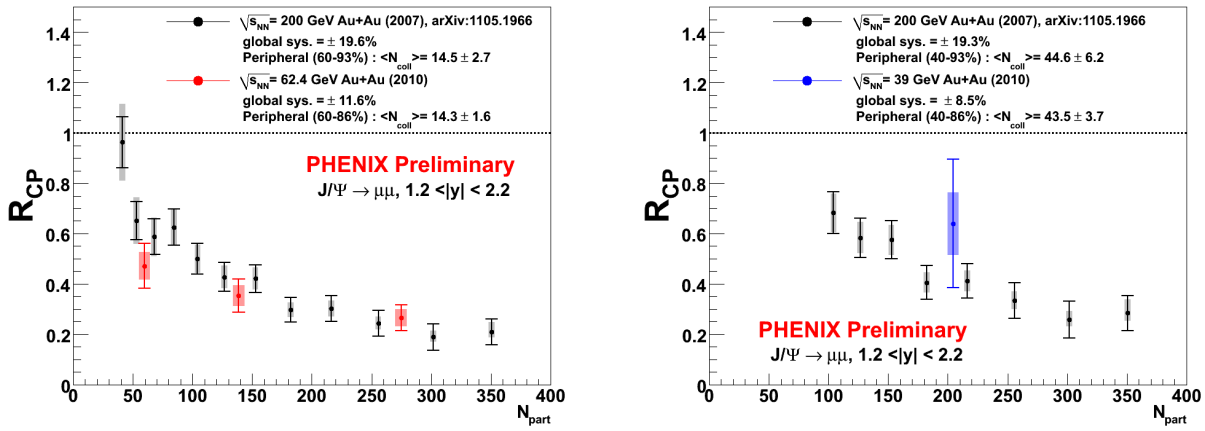

Figure 7: R_{CP} for J/ψ as measured in Au+Au collisions at $\sqrt{s_{NN}} = 200$, 62.4 and 39 GeV

3.3 Gluon polarization

The decomposition of the proton spin has been a long standing puzzle ever since first indications that the quarks only contribute to about 30% of the total proton spin. A sizable contribution from the gluons is a necessary ingredient making up the proton spin. Since an experimental determination of the partonic orbital angular momentum has so far not been established, the gluon polarization is an essential ingredient in our understanding of the proton structure. PHENIX has used double longitudinally polarized high energy p+p collisions to access the gluon helicity contribution ΔG in recent years. It has previously been shown that the (polarized) partonic cross sections at leading order are dominant for gluon-gluon fusion and quark-gluon scattering [20, 21].

PHENIX has measured double helicity asymmetries A_{LL} for different probes at center-of-mass energies $\sqrt{s} = 62.4\,\text{GeV}$ and $200\,\text{GeV}$ [3, 4, 10, 8]. Figure 8 shows our results for three runs at $\sqrt{s} = 200\,\text{GeV}$. These asymmetries in combination with jet results from STAR, inclusive, and semi-inclusive deep inelastic scattering (SIDIS) comprise the input for a NLO-pQCD analysis in order to extract the underlying polarized quark and gluon distributions [23]. Figure 9 summarizes the results of this analysis at $Q^2 = 10\ \text{GeV}^2$. We see that the gluon polarization seems to be small overall, but the uncertainties are still very large at low x (outside the accessible x-range at RHIC $0.05 < x < 0.2$). We would like to point out here that the vertical scale of the gluon polarization plot is larger than those for the sea quark polarizations. The determination of Δg at partonic momenta below 0.01 can therefore have significant implications for the total gluon contribution to the proton spin. The low-x region will become more important in pion production at $500\,\text{GeV}$ and can be tagged by certain combinations of meson correlations in the central and forward regions of the PHENIX detector. These measurements, combined with the existing ones at lower energy will allow meeting DOE-milestone HP12.

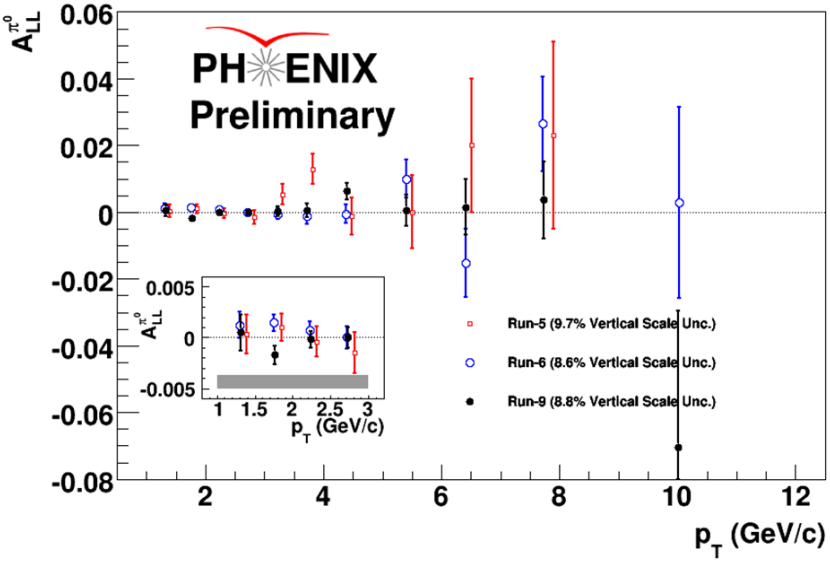

Figure 8: Double helicity asymmetry A_{LL} for neutral pions from runs 5, 6, and 9 as a function of transverse momentum p_T.

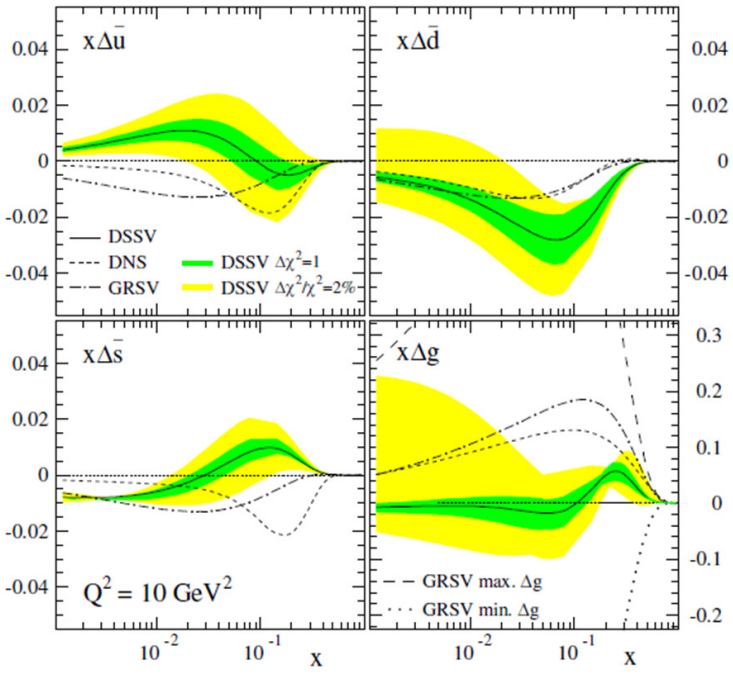

Figure 9: Polarized sea-quark and gluon distribution functions with uncertainty bands from a current NLO-pQCD fit to the world data of inclusive and semi-inclusive DIS and RHIC data by DSSV [23].

3.4 Sea quark polarization

As shown above, both the gluon and the sea quark polarizations are poorly constrained in the intermediate to low partonic momentum range ($x < 0.1$). Due to parity violating nature of the production of W-bosons, one can directly link the polarization of the initial state to the polarization of the involved quarks and antiquarks in the process. Together with different acceptances in forward or mid-rapidities, we will be able to probe the sea-quark polarization over a wide range of x without further involvement of fragmentation functions as required in SIDIS measurements [21].

In 2009, the first observations of single longitudinal polarized W-bosons from polarized p+p collisions at $\sqrt{s} = 500\,\mathrm{GeV}$ have been reported by both the PHENIX and the STAR collaborations[1, 15]. PHENIX used an integrated luminosity of $8.6\,\mathrm{pb}^{-1}$ with a proton beam polarization of 35% for beams. The analysis of the data was based on electrons from W decay in the central arm detectors. Since a full reconstruction of these events (including the decay neutrinos) is not possible, the analysis was aiming for the Jacobian peak of electrons with transverse momenta larger than $30\,\mathrm{GeV}/c$. Electron and positron candidates were carefully compared to background estimations from Monte Carlo generators (including smearing in the EMCal) and in data driven methods. The main contributions to the QCD background are charged hadron clusters and hadron decay photons which undergo conversion to electrons before the tracking system. Some are from a track misassociation in the same jet event. An isolation cut suppresses the background by about a factor of four. Figure 10 shows the cross section results of the world data in comparison with theory calculations. Figure 11 shows the results for the longitudinal single spin asymmetries for W- and Z-bosons as calculated from:

$$A_L = \frac{1}{P_{beam}} \cdot \frac{N^{\rightarrow} - R \cdot N^{\leftarrow}}{N^{\rightarrow} + R \cdot N^{\leftarrow}} \tag{1}$$

where $N^{\rightarrow}$ and $N^{\leftarrow}$ denote signal counts with positive and negative helicity of the polarized beam. A normalization for the relative luminosity R is applied to the counts before calculating the asymmetry. The error bars are from a maximum likelihood estimation for a 68% confidence level. The dominant systematic uncertainty is from conversion electrons in the detector material.

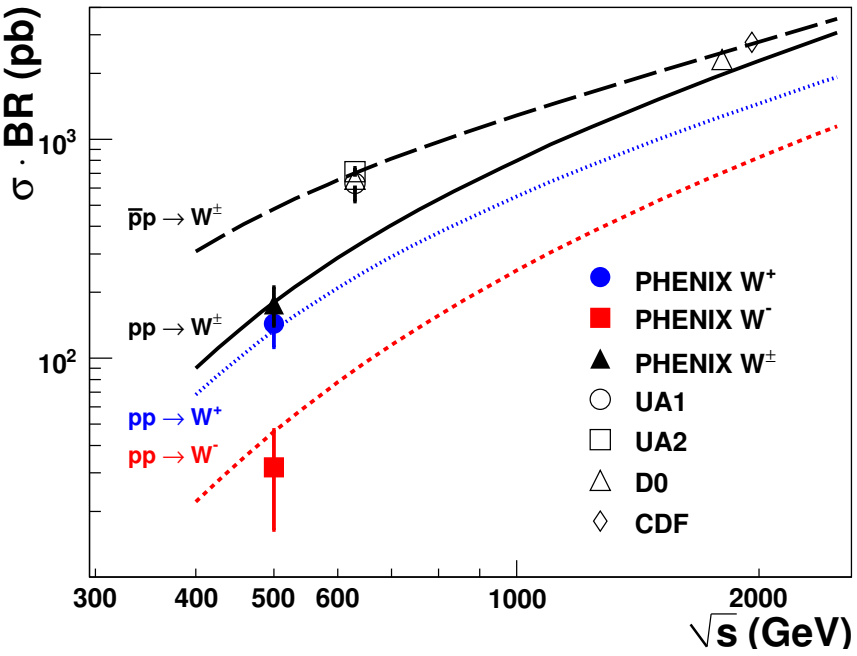

Figure 10: Inclusive W-boson cross sections for leptonic decays from PHENIX compared to world data and theoretical calculations.

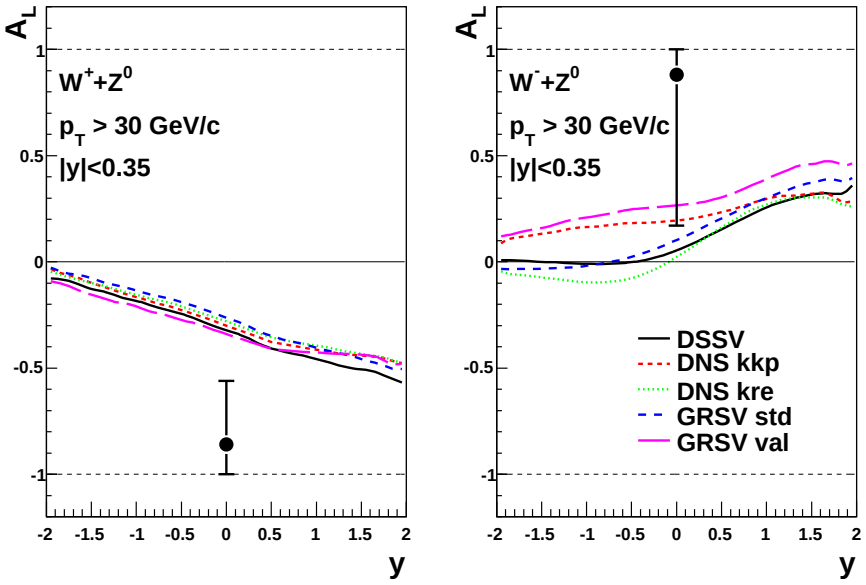

Figure 11: Longitudinal single-spin asymmetries for electrons and positrons from W and Z decays in the PHENIX central arm detectors.

3.5 Transverse single spin asymmetries

Large transverse single spin asymmetries have been a theoretical challenge in the past three decades. Predicted to vanish at high energies these asymmetries have persisted with significant amplitudes. Several mechanisms have been proposed to explain the measured asymmetries, including initial state correlations between the quark spin and the proton spin (Sivers effect [32]) as well as spin dependent fragmentation functions (Collins effect [22]) which can appear in combination with a non-vanishing transverse polarization of the quark (transversity). The transverse polarization of quarks is unknown too, since boosts and rotations do not commute in Lorentz transformations (in the highly relativistic parton motion). Phenomenological fits to SIDIS data to extract the Sivers function as well as the Collins fragmentation function from SIDIS and e^+e^- data have been made. In order to disentangle contributions from different effects, we will need a variety of measurements in different kinematic ranges and from different collisions systems as an input for a truly global analysis.

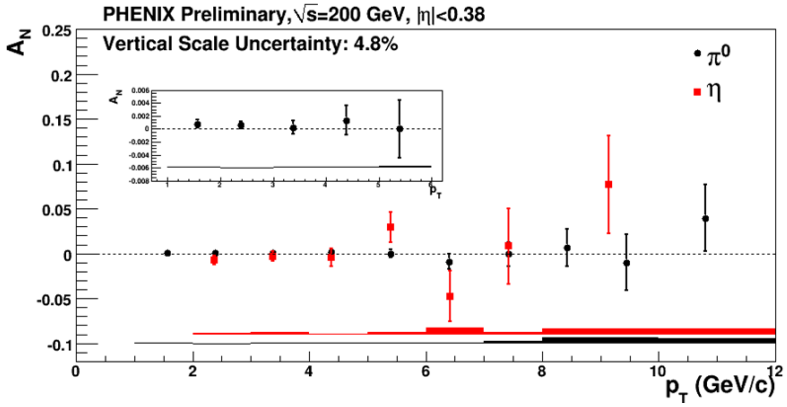

Figure 12: Transverse single spin asymmetries for pions and etas at mid-rapidity from the run 8 data set.

PHENIX has contributed transverse single spin asymmetries from its very first polarized data set for neutral pions and charged hadrons with the central arm detectors. Despite the statistical accuracy, these asymmetries have been used for a determination of the upper limit of the gluon Sivers function. In 2008, the π^0 single spin asymmetry, A_N, was determined from a data set with highly increased integrated luminosity and much improved beam polarization as compared to the previous measurement. Figure 12 includes the A_N of both π^0 and, for the first time, the A_N of η, as functions of the transverse momen-

tum p_T. The uncertainties are as small as 1/10% and all asymmetries are consistent with zero at mid-rapidities at $\sqrt{s} = 200\,\text{GeV}$. Large transverse single spin asymmetries have been observed in forward directions over a wide range of energies in the past decades ($\sqrt{s} = 4.9\,\text{GeV}$, 6.6 GeV, 19.6 GeV, 62.4 GeV).

PHENIX used a newly commissioned electromagnetic calorimeter (Muon Piston Calorimeter, MPC) at pseudo-rapidities $3.1 < \eta < 3.9$ during the 2008 RHIC run for the measurement of inclusive cluster asymmetries. The geometry and position of the MPC is such, that clusters from neutral pion decay photons start to merge at pion energies below 20 GeV. Detailed event generator studies (PYTHIA) combined with a full detector simulation show that the clusters in the MPC are dominated by π^0 decays. Contributions from other mesons and direct photons are generally less than 10% in this kinematic range.

Figure 13 shows the results of the inclusive cluster asymmetries as a function of p_T for both forward ($x_F > 0$) and backward ($x_F < 0$) going particles (the direction of the polarized beam defines the forward direction in this case). Backward asymmetries are consistent with 0 as expected. Forward asymmetries rise with p_T. This behavior is especially interesting, because in the transition region of of the phenomenological description of TMD parton distribution functions ($q_T \ll Q^2$) to a collinear twist-3 picture ($q_T \approx Q^2$), the asymmetry is expected to fall off again [27]. We may see a hint of this behavior, but the asymmetries at large transverse momenta clearly need a more solid basis in terms of statistics.

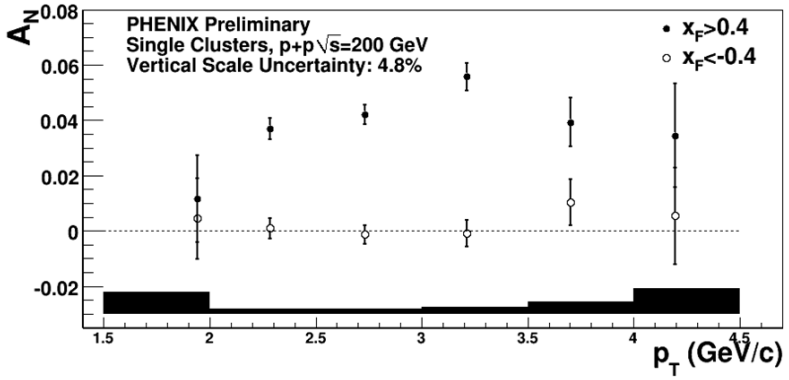

Figure 13: Cluster transverse single spin asymmetries in the MPC for forward and backward going particles.

4 Upgrades accomplishments

4.1 HBD analysis

The 2010 run was the second and last of two runs featuring the PHENIX HBD detector. The HBD is a unique cutting-edge technology and was found to work exactly in accord with its design specifications. The HBD is a windowless Čerenkov Detector that takes advantage of the exceptional transparency of CF_4 gas (down to $\lambda = 108\,\text{nm}$) and the $1/\lambda^2$ yield of Čerenkov light to produce an exceptional yield of Čerenkov light per unit distance. The yield of Čerenkov light accounting for all factors (gas transparency, mesh transmission, active area, etc) was anticipated and measured to be 22 photo-electrons.

It is only by virtue of this large photoelectron yield that small angle pairs resulting from Dalitz decay and photon conversions can be identified and rejected from further analysis. Indeed, the $N_0 = 330$ is the highest ever recorded for a Čerenkov detector. Furthermore, the quantum efficiency (measured in situ) was maintained throughout the two years of operation of the HBD in PHENIX. During the 2010 run, the HBD started with 95% active area and ended with an active area of 95%. Overall the detector performance was superb.

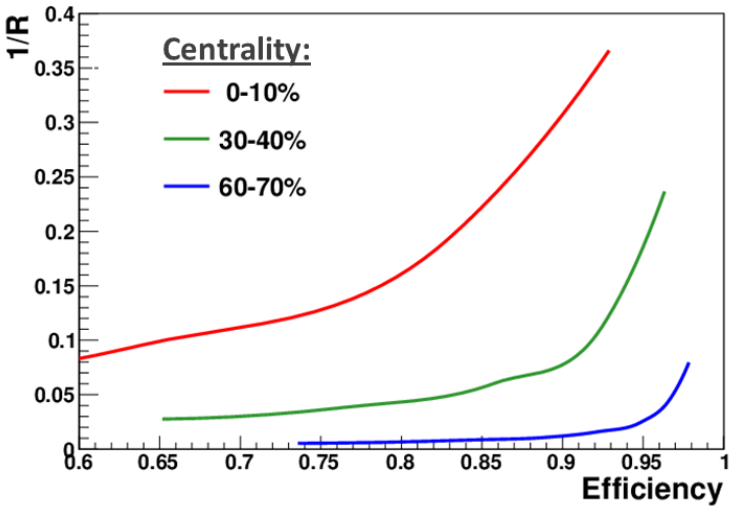

Figure 14: Čerenkov light yield in the HBD.

CF_4 gas produces scintillation light. Although the was used for the positive benefits of continual gain measurement and occasional quantum efficiency measurement, the draw-

back is the large scintillation light yield during central collisions. As anticipated, this scintillation light has proved to be among the most challenging aspects of dielectron analysis with the HBD. A background to electrons tagged by the HBD is created from random coincidences of scintillation photons with downstream conversion electrons detected in the PHENIX central arms. Two independent algorithms for dealing with scintillation background were developed and both were successful. Figure 14. indicates the rejection against fake electron signals (plotted here as $1/R$) as a function of the electron efficiency for one of the algorithms. As indicated, the rejection of scintillation background remains high with reasonable electron efficiency.

A summary of the performance of the HBD in the face of this background is given in the table below. As indicated, in central collisions a singles efficiency of 83% is retained with a background rejection of 3.5. In terms of pairs, this results in an overall S/B improvement of 8.4, close to the design goals for HBD performance. Results on the background subtracted dielectron spectrum are not yet complete, but are anticipated in the near future.

Origin of electrons	Electrons/ event Central Arms	Electrons/ event Central Arms + HBD	Efficiency	Rejection
Signal	0.17	0.14	**0.83**	
Downstream convers.	0.85	0.09		**9.7**
Misidentified hadrons	0.33	0.07		**4.7**
Other electrons	0.22	0.15		**1.5**

Figure 15: Summary of various aspects of the HBD performance.

VTX installation and commissioning

The installation and commissioning of the VTX in Run-11 marks the successful completion of the first phase of a major upgrade to the capabilities of PHENIX. The VTX consists of two layers of pixels surrounded by two layers of stripixels. The nominal radii of the four layers from the beam line are 2.5 cm, 5 cm, 11 cm, and 16 cm, respectively. The detector covers $|\eta| < 1$ in pseudo-rapidity and $\Delta\phi$ of 80% of 2π in azimuth. The detector can measure vertex position of a track with a precision of 50 μm to 100 μm. The high precision will enable us to separate decay electrons from B and D mesons. The detector also provides large solid angle stand-alone tracking with modest momentum resolution ($\delta p/p \simeq 5\% \oplus 10\% p$).

The VTX was completed in the middle of November 2010, and its installation into PHENIX IR was completed December 1, 2010, in time for the start of Run-11. It was commissioned during the 500 GeV p+p run, collecting some 5×10^6 events. The VTX performed very well, with extremely low noise hit rate in the pixel detectors and good S/N ($\simeq$ 11) for the stripixel detectors. At the time of installation, approximately 97% of the channels are operating. Figure 16 shows a picture of the VTX installed in PHENIX.

The main purpose of the VTX is to identify the displaced vertices of D and B meson decays, allowing the separate identification of open charm and open beauty. Surveys performed during construction located the individual VTX silicon detectors to a resolution of approximately 35 μm, implying that the Day-1 performance goal of distance-of-closest approach (DCA) resolution of 100 μm should be readily achievable. This resolution is sufficient for RUN11 physics goal of b/c separation. After detector alignment using the beam data, the detector should achieve DCA resolution of 50 μm for high p_T ($p_T > 2$ GeV/c) tracks. This is supported by a measurement of the transverse size of the beam, as shown in the left panel of Figure 17. Here we show the distribution of the y-projection of tracks on x=0 plane. These tracks are high momentum tracks in 500 GeV p+p reconstructed in a small part of the VTX. The width of the distribution is 95 μm. Based on the emittance and β^* of the beam, the beam spot size is expected to be 85 μm (1D) for 500 GeV p+p. These two values for the beam spot size are entirely consistent. This implies that a DCA resolution much better than 100 μm is achievable after over-all detector alignment using beam data.

The right two panels of Figure 17 illustrate the functioning of the VTX in both p+p and Au+Au collisions. The VTX is currently taking data in Au+Au collisions. The concur-

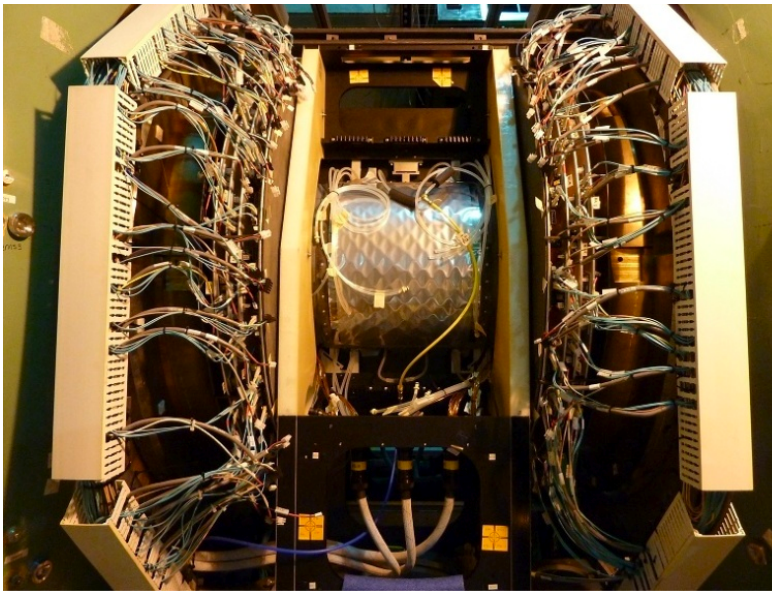

Figure 16: A picture of the VTX installed in PHENIX. The complex installation involved routing the far-side half of the VTX under the beam pipe and then tipping it up vertically into position.

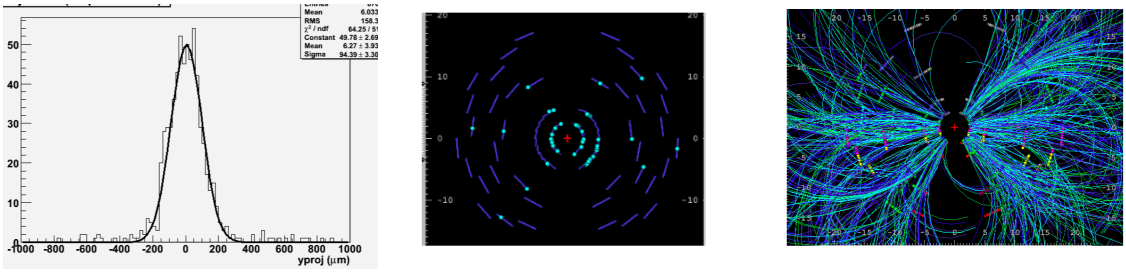

Figure 17: Illustrations of the VTX performance during Run-11. (left) A reconstruction of the p+p beam spot size. The 95 μm reconstructed size agrees well with the expected beam spot size of 85 μm. (middle) Hits in the VTX for a p+p event. (right) Reconstructed tracks in the VTX in a Au+Au event.

rent improvements in the DAQ and successful implementation of zero suppression in the read-out of the VTX have allowed PHENIX to retain its very high DAQ rate of better than 5 kHz in Au+Au. We expect that we will record several billion events of 200 GeV Au+Au data by the end of RUN11.

4.2 Muon trigger upgrade for W physics

The PHENIX muon trigger upgrade for W physics has two principal components: additional trigger cards for the front-end electronics of the muon tracking chambers, MuTr, (JSPS funded) and resistive plate chamber detector stations, RPC-1 and RPC-3, with their front-end electronics (NSF funded). The MuTr trigger front end boards send data via optical fibers to new transition boards (merge boards, JSPS funded) where signals are reformatted for each of the muon spectrometer octants. The octant based signals are bundled with RPC signals and are sent to FPGA trigger processor boards (local level-1 (LL1), NSF funded).

Trigger decisions in the LL1 are based on matching high momentum MuTr tracks with hits in the RPCs. The timing information from the RPCs is used to reject beam backgrounds in the trigger decision. The muon trigger upgrade team consists of 90 PHENIX collaborators from 18 institutions in China, Korea, Japan and the USA.

In the offline W analysis the trigger timing from the RPCs will be used to remove cosmic ray backgrounds and to connect muon tracks with the correct bunch crossing and, therefore, with the correct beam polarization information for the event. In addition to the muon trigger upgrade, W physics in the muon spectrometer arms requires two additional stainless steel absorbers for the suppression of low momentum hadrons that otherwise decay and are incorrectly reconstructed (in combination with their decay muons) as high p_T tracks. Two new hadron absorbers were funded with contributions from RIKEN, BNL, NSF and UIUC and were manufactured by ATLAS Tool & Die in Illinois. Figure 18(a) shows the installation of absorber plates on the back-side of the central magnet yoke upstream of the north muon spectrometer in September 2010.

The trigger cards for the MuTr front-end, RPC-3 north and the merge boards were installed before Run-10. RPC-3 south and the LL1 trigger processors were added in October and November, 2010, completing the first integration stage of the muon trigger. Figure 18(b) shows a snapshot of the RPC-3 south installation in the RHIC beam tunnel in November, 2010. Figure 18(c) shows the merge boards with all optical fibers to the MuTr and the LL1 connected and Figure 18(d) displays the LL1 trigger processor crate.

The second integration stage of the trigger will include the two upstream RPC-1 stations which will increase the trigger rejection to the level needed for the highest luminosities in future $p+p$ running at RHIC. An RPC-1 prototype was installed for Run-11 for rate

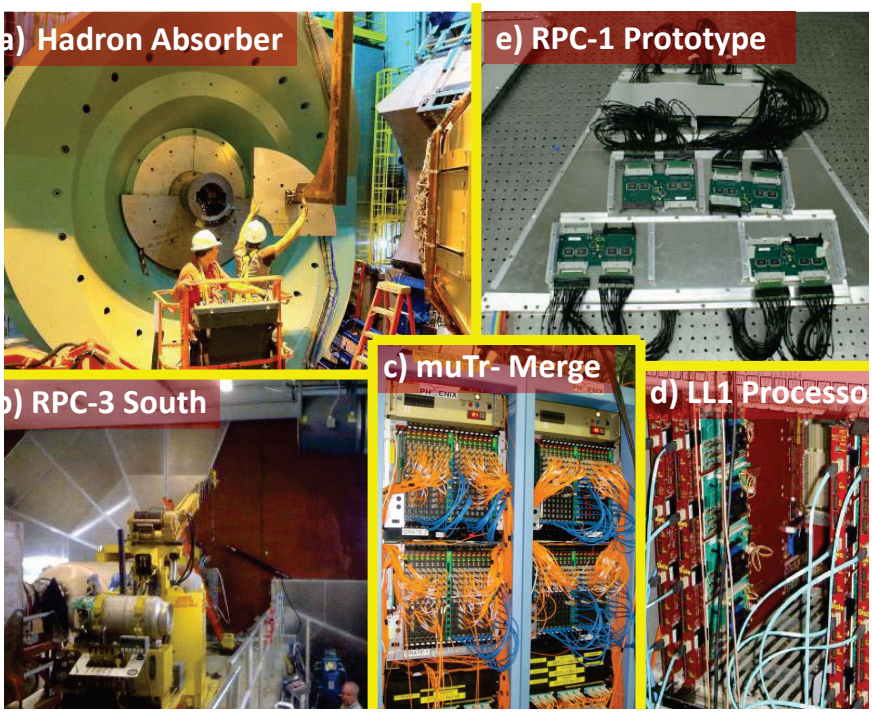

Figure 18: a) Installation of the north hadron absorber. b) Installation of RPC-3 south. c) The MuTr merge boards. d) The LL1 trigger processors. e) The latest RPC-1 octant prototype.

and background tests. Figure 18(e) shows the latest RPC-1 octant prototype. The RPC-1 detector assembly is scheduled to be carried out from June to August, 2011, and the installation of RPC-1 is scheduled for August and September, 2011.

PHENIX carried out a 10 week long run with polarized protons at $\sqrt{s} = 500\,\text{GeV}$ for W physics from January to April 2011. The average beam polarization was $\langle P \rangle = 0.45$ (from online analysis) and the recorded integrated luminosity was $30.6\,\text{pb}^{-1}$ before cuts on the vertex distributions. The muon trigger systems were commissioned successfully and about $25\,\text{pb}^{-1}$ of the data sample were recorded with all the MuTr triggers systems operational and the RPCs read out in the offline data stream. The muon trigger used during the run was the new MuTr trigger in coincidence with the usual beam-interaction trigger (without vertex cut) and the usual muon identifier trigger: MuTr $\cap$ BBC(no vertex) $\cap$ MuID. The rejection of the muon trigger was 5000 for a collision rate of BBC(no vertex) $= 0.5$ MHz decreasing linearly to 1200 at BBC(no vertex) $= 3.0$ MHz. The muon trigger was not pre-scaled and has sampled the full $25\,\text{pb}^{-1}$. RPC timing information is available for the offline data analysis. A hit frequency distribution vs position is shown for RPC-3 north in Figure 19-a and the results of RPC efficiency from a high

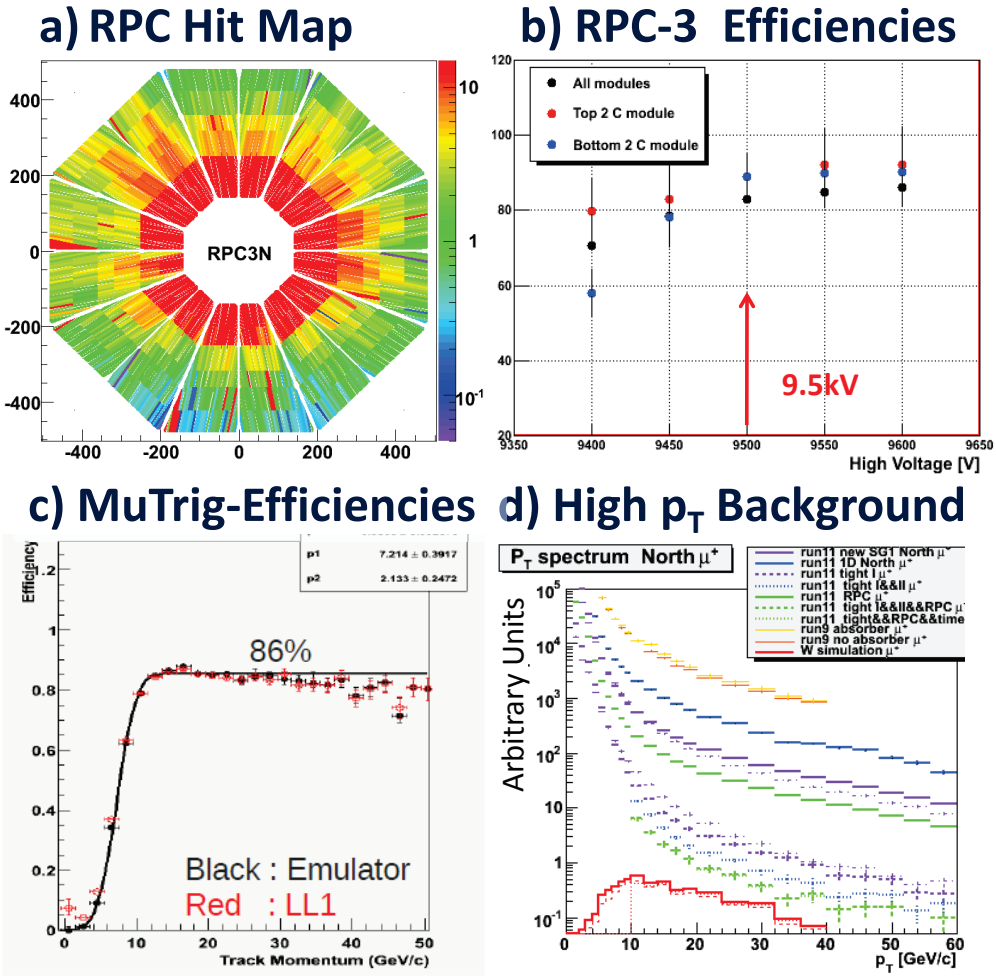

Figure 19: a) RPC-3 north hit distribution vs position in [cm]. b) RPC-3 relative efficiencies - not corrected for hadrons reconstructed in the MuTr but not passing through the MuID steel to RPC-3 (leading to lower efficiencies). c) LL1-south efficiencies with respect to MuTr hits and trigger emulator prediction vs momentum. d) Offline analysis: Single muon spectra vs p_T for different track selections compared to the spectrum expected for muons from W-decay (red line).

voltage scan are shown in Figure 19-b.

Parallel to the data taking the RPC*MuTr trigger (without the BBC and the MuID coincidence) was commissioned and operated successfully during the last week of the p+p run. With RPC timing cuts turned on the RPC*MuTr trigger reached a rejection power of 1100 at a collision rate of BBC(no vertex) $=$ 2.7 MHz. Additional improvements in

rejection power will result from the introduction of RPC-1, shielding of RPC-3 from outgoing beam backgrounds, optimized timing cuts in the RPCs, completing proper anode grounding work of MuTr chambers and narrow roads in matching outgoing MuTr tracks with RPC hits in the LL1 trigger algorithm. We expect an improvement of a factor 5 to 10.

A fast turn-around data production was carried out to monitor the performance of the trigger systems based on detailed offline analysis: detector and trigger efficiencies were found to be consistent with expectations. For example, Figure 19-c compares the MuTr LL1 trigger efficiency with the efficiency predicted by a trigger emulator running on data written to disk. The trigger is fully efficient for muon momenta above $14\,\mathrm{GeV}/c$. The full $25\,\mathrm{pb}^{-1}$ have been processed in fast data production and first offline analysis has started. For example, initial results on single high p_T muon spectra are shown for different sets of cuts in Figure 19-d. For $p_T > 20\,\mathrm{GeV}/c$ and with tight background rejection cuts the observed spectrum comes close to the expected signal spectrum of muons from W decay (red line in Figure 19-d). At this very early stage in analysis the signal to background ratio is found to be $S/B \approx 1/2$. Improved alignment and tracking in the MuTr and the optimization of cuts rejecting high p_T backgrounds will improve the S/B ratio, aiming to reach $S/B \approx 3/1$.

4.3 DAQ Upgrades

Integration of the silicon vertex detectors into the data acquisition system required a significant upgrade of data acquisition electronics. In order to record events at rates of 6 kHz with the addition of a potentially large quantity of data from the vertex detectors (about 1.7 Mbyte/event before zero suppression from the barrel, added to approximately 0.15 Mbyte/event of zero suppressed data from the rest of the detector), new Data Collection Modules (DCM II's) were designed to receive data transmitted at 1.6 Gbit/s from the Front End Modules using the TI TLK2501 serializer/deserializer on approximately 100 optical fibers. Data from groups of DCM II's were buffered and aggregated for transmission over fiber to six sub-event buffer computers (SEB's) with a new four lane PCIe interface, for transmission over a 10 Gbps Ethernet network which was upgraded for this purpose. Much of the acquisition was carried out in firmware in FPGA's on the DCM II and interface boards, but a very significant software effort was necessary to integrate the new hardware into the Event Builder and data archiving systems by data acquisition groups at Columbia University, the University of Colorado, and the Physics Department at Brookhaven National Laboratory, in configuration of the detector electronics, moni-

toring and equipment protection, and additional data logging speed necessitated by the larger data volume.

5 Beam use proposal for Run-12 and Run-13

The Associate Laboratory Director for Nuclear and High Energy Physics has directed the experiments to plan assuming 26–30 weeks in Run-12 and 26 weeks in Run-13, clearly stating our priorities to give guidance should the run be shorter. Detailed guidance provided by the Collider-Accelerator Department (C-AD) describes the projected year-by-year luminosities for various species, along with the expected time development of luminosity in a given running period [36]. We have used the species dependent luminosity guidance, the stated cool-down time, and the stated start-up and ramp-up time for each species to convert the required delivered integrated luminosities into a plan for the approximate number of weeks at each species. We also take into account an additional week of set-up to develop polarization in 500 GeV $p+p$ collisions.

Based on the C-AD guidance, not updated since the time of last year's PAC meeting, we assume the following for luminosities and polarization (please see below for explanation of the difference between delivered and recorded or sampled luminosity):

- Based on our experience to date with $p+p$ collisions at $\sqrt{s} = 500\,\mathrm{GeV}$, we assume that our goal of $100\,\mathrm{pb}^{-1}$ delivered can be reached in 8 weeks. The integral is attainable with 10 successful stores per week.
- Our plan for 500 GeV p+p running is based on the projected polarization of 50% for run 12 and 60% for run 13. Should this not be attained after 4-5 weeks of physics running, we anticipate that the goals and run length may be re-optimized.
- After the ramp-up period, average Au+Au delivered luminosity per week at $\sqrt{s_{NN}} = 200\,\mathrm{GeV}$ is $990/\mu\mathrm{b}$ in Run-12.

In order to determine the fraction of delivered luminosity that can be recorded by PHENIX, we utilize the following factors:

- The PHENIX live-time is taken as 97%, which is the same as that in recent Runs. We anticipate maintaining this factor also in p+p.
- The PHENIX up time is taken to be 65%, commensurate with recent data taking with full energy Au+Au.
- Our planning assumed 20% of the p+p collisions inside ± 10 cm and 55% inside ± 30 cm. 25% of Au+Au collisions at $\sqrt{s_{NN}} = 200$ GeV are assumed to be inside ± 10 cm.

For most of the polarized p+p and full energy Au+Au running, the projected collision rates are sufficient to reach the PHENIX bandwidth limit. Consequently, we will trigger primarily on rare processes in p+p (e.g. high momentum leptons and photons) and implement several vertex cuts at the trigger level for Au+Au data taking. In Au+Au at 200 GeV, we will employ, in addition to minimum bias triggers, a mix of high p_T photon and electron triggers. We also anticipate utilizing muon triggers once we see that sufficient rejection power is achieved with the new shielding installed for the W program.

The physics performance studies for Run-12 have been done under the following assumptions: 300 pb^{-1} delivered integrated luminosity in 8 weeks of physics data taking for 500 GeV p+p. This yields 100 pb^{-1} sampled inside a vertex of ± 30 cm for the W measurements in the muon arms via

$$(\text{PHENIXlive} = 0.97) \times (\text{PHENIXup} = 0.65) \times (\text{vertex} = 0.55) = 0.35\% \qquad (2)$$

It may be found that events outside a 30 cm vertex cut can be successfully utilized. However until that is demonstrated with data, we plan the running time assuming a 30 cm vertex cut. In full energy Au+Au we assume data taking at an average data acquisition rate of 2.5 kHz, to account for the commissioning of the FVTX, though we anticipate that the maximum possible data taking rate will be nearer to 5 kHz. The higher rate is consistent with early experience coming from Run-11. Using the information in [36], the PHENIX projected luminosities are calculated incorporating a realistic ramp-up time, as detailed in [36], and the mean value of the maximum and minimum luminosity projections for each year's running period.

The PHENIX Beam Use Proposal is summarized in Table 1. The proposed program follows the strategy laid out in the PHENIX Beam Use Proposal presented last year. It is consistent with the PHENIX decadal plan submitted on October 1, 2010 [19], with changes that primarily reflect the realities of the currently ongoing Run-11. We note that the proposed order of the species, as shown in the table, is not identical to the priority assigned

Table 1: Baseline PHENIX run plan for Run-12 and Run-13. Longitudinal polarization is indicated by (L), transverse by (T).

run	species	$\sqrt{s_{NN}}$	weeks	$\int$ L dt		pol.	comments
				$\lvert z\rvert < 30$ cm	$\lvert z\rvert < 10$ cm		
12	p+p	200	5	13.1 pb^{-1}	4.7 pb^{-1}	60% (T)	HI comparison, $\perp$ spin
	p+p	500	8	100 pb^{-1}	35 pb^{-1}	50% (L)	W program + ΔG
	Au+Au	200	7		0.8 nb^{-1}		heavy flavor (F/VTX)
	U+U	193	1.5		0.03 nb^{-1}		explore geometry
	Au+Au	27	1	5.2 μb^{-1}			energy scan
13	p+p	500	10	200 pb^{-1}	74 pb^{-1}	60% (L)	W program
	p+p	200	5	20 pb^{-1}	4.7 pb^{-1}	60% (T)	HI comparison
	Cu+Au	200	5		2.4 nb^{-1}		control geometry
	U+U	193	5		0.57 nb^{-1}		explore geometry

by the collaboration to the physics. For practical reasons, we request that 200 GeV p+p precedes the higher priority 500 GeV p+p. This is to allow commissioning the RPC1 detectors with beam prior to the start of the W data taking. We also anticipate benefits to the polarization by allowing CA-D to separate start up of RHIC from optimizing the polarization. Running p+p before ions will allow PHENIX to commission the FVTX with beam prior first Au+Au running. In case the budget in FY12 allows for 30 cryo weeks, PHENIX proposes modifying the above plan with the steps enumerated below; time modification to the running schedule proposed in Table 1 are listed in PHENIX priority order.

- Add 62.4 GeV p+p for 1 week
- Add 39 GeV p+p for 1 week

- Lengthen 27 GeV Au+Au from 1 week to 2 weeks.

5.1 Run-12

The twin top priorities for PHENIX in Run-12 are polarized proton running to make progress toward our spin physics goals, and full energy Au+Au running to utilize the new FVTX and VTX detectors to separate charm and bottom in heavy ion collisions. The 200 GeV p+p serves as a reference run for the VTX data collected in Run-11 and Run-12, and provides transverse spin physics. It is our next highest priority for Run-12.

The commissioning of the FVTX detectors will begin during the 200 GeV $p+p$ portion of Run-12. Because this is the first run of this major new detector system, the FVTX will most likely not provide physics quality data for 200 GeV $p+p$ collisions in Run-12. How rapidly the detector commissioning proceeds will determine whether good physics data will be available from the FVTX for any part of the 200 GeV Au+Au run. At this time, we assume that the bulk of the high Quality FVTX physics data for both $p+p$ and Au+Au will be collected in runs 13 and 14.

We anticipate beginning the study of U+U collisions during this running period, as the program was not able to be initiated in Run-11. Consequently, as our fourth priority, we request an initial small U+U data set in Run-12, to be collected as part of commissioning uranium beams in the new EBIS source. This will allow development of analysis methods to demonstrate control/selection of the geometry of collisions in this non-spherical system, event by event. As this utilizes observables with large cross section, a small number of events will suffice for the initial study. Once we have demonstrated the ability to fully exploit the unique features of U+U collisions, we will need a much larger data set to allow the study of hard probes; we anticipate this longer run to take place in Run-13.

Our fifth priority is to fully exploit the energy scan data collected in Run-10. This necessitates collecting reference $p+p$ data at several low energies, and collecting a substantial set of data with Au+Au collisions at $\sqrt{s_{NN}} = 27$ GeV. In order to fully utilize the energy scan data collected at 62 and 39 GeV in Run-10, we request p+p collisions for comparison at the same energies.

5.1.1 Spin physics goals for Run-12 and Run-13

The spin physics goals in PHENIX for runs 2012 and 2013 are measurements of quark and anti-quark helicity distributions through parity violating longitudinal single spin asymmetries, A_L in W-production and measurements constraining the gluon spin contribution to the proton spin in the range $0.01 < x_g < 0.3$. These measurements will address the goals defined by NSAC milestones HP8 and HP12.

In addition to the data taking with polarized protons at $\sqrt{s} = 500\,\text{GeV}$, PHENIX proposes to acquire two data samples at $\sqrt{s} = 200\,\text{GeV}$ as reference sample for the heavy flavor measurements with the new vertex detectors in heavy ion collisions. For the spin physics program the resulting data sample will be used for precision measurements of single transverse spin asymmetries, A_N, at high p_T and forward rapidity. It is also planned to carry out exploratory measurements of single spin asymmetries A_T that isolate contributions from the Collins effect and the Sivers effects.

The proposed program is consistent with and follows the PHENIX decadal plan submitted on October 1, 2010 [19].

5.1.2 Assumed beam conditions and experimental readiness

The assumptions with regards to integrated luminosity and polarization used in the PHENIX run plan are based on guidance from the Collider Accelerator Department. For $\sqrt{s} = 500\,\text{GeV}$ PHENIX proposes a 8 week long run in 2012 and a 10 week long run in 2013. This will lead to a total data sample of $\int Ldt = 300\,\text{pb}^{-1}$ with an average polarization of $P = 0.55$. This data sample will make it possible to achieve the W-physics goals outlined in the PHENIX Decadal Plan. Additional running beyond 2013 would be scheduled if the performance goals could not be meet during the 2012 and 2013 runs.

Two 5 week long p+p runs with $\sqrt{s} = 200\,\text{GeV}$ runs in 2012 and in 2013 will result in a data sample of $\int Ldt = 33\,\text{pb}^{-1}$ with a beam polarization of $P = 0.6$.

PHENIX has commissioned successfully the new muon trigger for physics with W-bosons during run 11. A first physics run was completed in April 2011 with about $\int Ldt = 18\,^{-1}$

within vertex cuts of $|z| < 30\,\text{cm}$. The trigger rejection of the new muon trigger was sufficiently high to sample the full delivered luminosity. An additional muon trigger RPC station[1] will be installed in the summer of 2011. The additional detector station in combination with reduced backgrounds, optimized timing cuts and improved position correlations will ready the muon trigger for the highest luminosities projected by CAD for the W-physics program.

Two 12 ton absorbers were installed upstream of the muon spectrometers for run 11 and serve successfully the rejection of offline backgrounds at high p_T in the W analysis. The run 11 data sample acquired with the new muon trigger were fast produced in nearly real time and first offline analysis finds a signal to background ratio of $S/B = 1/2$. Improved alignment and tracking in the muon tracking chambers and the optimization of cuts will further improve the signal to background ratio. For runs 12 and 13 it is expected that the signal to background ration will be between $1 < S/B < 3:1$.

The highest sensitivity for gluon spin measurements at low x require excellent control of all systematic uncertainties. In particular the uncertainty in the relative luminosity measurement needs to be reduced to below 10^{-4} to fully take advantage of the large data sample for accessing small asymmetries. For example, the gluon spin distribution, $\Delta G(x)$ from the so-called minimal DSSV set leads to asymmetries of about 2×10^{-4} at low p_T for inclusive double spin asymmetries for electromagnetic clusters in the MPC. Possible improvements of the relative luminosity analysis are presently under study using run 11 data. However, reducing the relative luminosity uncertainty by a factor 5-10 may require a new relative luminosity monitor. An idea to use a single arm LT has been tested in run 2004.

In summary, PHENIX has demonstrated readiness for its W physics program in the past run 11. An improvement by a factor $5-10$ in the relative luminosity measurement will be needed to fully use the high luminosity run for W physics for precision measurements of $\Delta G(x)$ at small x. An effort is underway to improve the uncertainties in relative luminosity prior to run 12.

[1] A full size prototype for RPC-1 was tested in PHENIX successfully during run 11.

5.1.3 Summary of the physics goals in p+p

- The determination of quark and anti-quark helicity distribution through measurements of inclusive A_L^{μ} and A_L^{+e} in W-boson production with an integrated luminosity of $\int Ldt = 300\,\mathrm{pb}^{-1}$ and an average beam polarization of P=0.55 in polarized proton-proton collisions at $\sqrt{s} = 500\,\mathrm{GeV}$. About $\int Ldt = 120\,\mathrm{pb}^{-1}$ with P=0.50 will be available in time to satisfy NSAC milestone HP8 for 2013.

- Measurement of the gluon spin contribution to the proton spin for $0.01 < x_g < 0.3$. This goal is the NSAC milestone HP12 for 2013 and will be reached in PHENIX through measurements of inclusive double spin asymmetries for neutral pions at mid-rapidity, $|\eta| < 0.35$ and forward rapidity $3.1 < \eta < 3.9$, as well as measurement of di-hadron pairs with the trigger hadron either a mid-rapidity or forward rapidity and the associate hadron at forward rapidity. This measurement will be carried out in parallel to the W measurements with $\int Ldt = 300\,\mathrm{pb}^{-1}$ and P=0.55.

- Precise measurements of A_N for pions at forward rapidity and at high p_T and first measurements of single transverse asymmetries A_T probing directly the Collins effect or the Sivers effect in polarized proton-proton collisions. These measurements will be using a data sample of p+p collisions at $\sqrt{s} = 200\,\mathrm{GeV}$ with $\int Ldt = 33\,\mathrm{pb}^{-1}$ and $P = 0.6$ that also will serve as comparison data sample for heavy flavor physics in heavy ion collisions.

5.1.4 Physics with W-Bosons (HP8, 2013)

The highest priority for PHENIX Spin for Run-12 and Run-13 is to complete the 500 GeV longitudinal spin program. This plan requires sampling $300\,\mathrm{pb}^{-1}$ at PHENIX, which implies the delivery of approximately $900\,\mathrm{pb}^{-1}$ to our interaction point. These data will enable us also to independently constrain the ratio $\overline{d}/\overline{u}$ without the assumption of charge symmetry. Finally, the data sample allows for measurements of the gluon spin polarization in the proton down to x 0.01.

It is imperative to collect sufficient data before 2013 to achieve NSAC milestone HP8, which requires measurement of flavor-identified q and $\overline{q}$ contributions to the spin of the proton via the longitudinal-spin asymmetry of W production in calendar year 2013. We anticipate that this milestone can probably be at least partially satisfied with with the

requested luminosity for run 2013; the ultimate result will require 900 pb^{-1} delivered luminosity.

5.1.5 $\Delta\overline{u}, \Delta u, \Delta\overline{d}, \Delta d$

The parity-violating asymmetry $A_L^{W^\pm}$ in the production of $W^\pm$ bosons permits the determination of the light quark and light antiquark polarizations in the proton. In PHENIX this will be done via the detection of high p_T electrons/positrons in the central arms from the decay $W^\pm \to e^\pm\nu$ and of high p_T muons in the muon arms from $W^\pm \to \mu^\pm\nu$. Our simultaneous coverage in forward, backward, and central rapidity will provide a powerful means of determining the quantities $\Delta\overline{u}/\overline{u}$, and $\Delta\overline{d}/\overline{d}$ in the parton momentum range $0.05 < x_{Bj} < 0.6$. Almost direct quark/anti-quark separation is possible with forward/backward leptons from W^- production in the PHENIX muon arms due to much larger quark density vs anti-quark density at large momentum transfer. In this case, $A_L(\text{forward } W^- \to \mu^-) \approx \Delta d/d$. Similarly, $A_L(\text{backward } W^- \to \mu^-) \approx \Delta\overline{u}/\overline{u}$. Additionally, measurement of W^+ production will give access to $\Delta u/u$ and $\Delta\overline{d}/\overline{d}$. However, due to the fixed neutrino helicity, the flavor contributions in forward and backward rapidity are mixed. Similarly, the parity-violating asymmetry of W^+ production in central rapidity combines contributions from both u and $\overline{d}$ polarizations, and from d and $\overline{u}$ polarizations in W^- production. These measurements will have their greatest impact in improving global fits that seek to determine the polarized parton distribution functions in the proton.

Figure 20 shows our expectations, assuming 55% polarization, for the asymmetry uncertainties with 300pb^{-1} sampled in the muon channel (left panels) and electron channel (right panel). The curves show the calculated single spin asymmetries based on quark and anti-quark helicity distributions from different pQCD fits to inclusive and semi-inclusive DIS data along with RHIC polarized p+p data from previous runs. For the muon channel we have assumed that a S/B=3 can be reached for runs 12 and 13. The projections for the electron channel are based on the published result from run 9 and take into account the additional background created by the material in the newly installed silicon vertex detector.

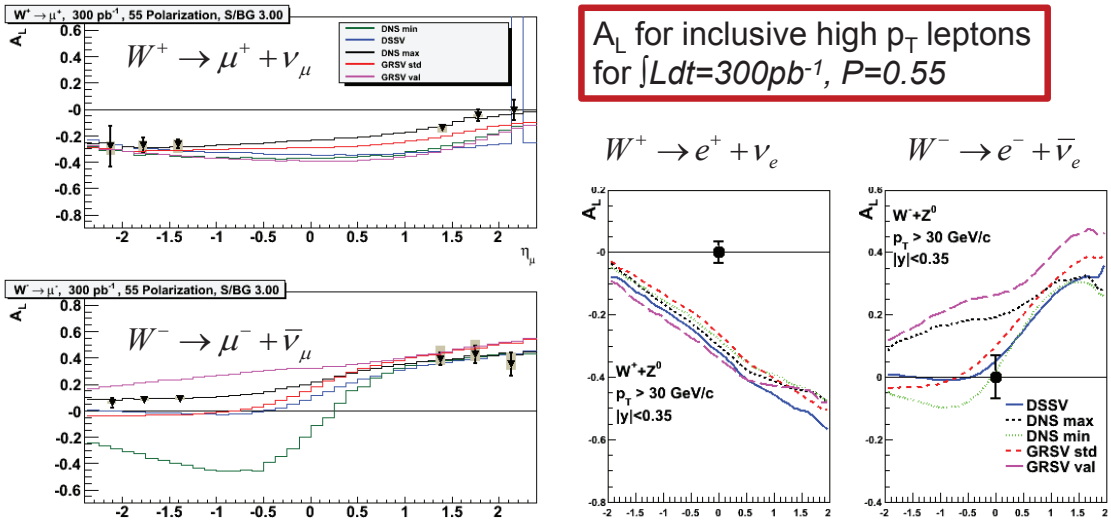

Figure 20: Expectations for the uncertainties in the parity violating inclusive single spin lepton asymmetry $A_L^{\mu,e}$ from W-production. The left side shows projections for the muon channel and the right side shows projections for the electron channel for $\int Ldt = 300\,\mathrm{pb}^{-1}$ and $P = 0.55$. For the muon channel as signal to background of $S/B = 3/1$ was assumed. The projections shown for muons are based on detailed simulations including full detector response and inclusion of all backgrounds. The projections shown for electrons are based on the published PHENIX result from run 2009.

5.1.6 $\bar{d}/\bar{u}$ ratio from W-production in PHENIX

The ratio $R = \sigma^{W^+}/\sigma^{W^-}$ of cross sections for W^- and W^+ production in p+p collisions at RHIC provides a new way to measure the asymmetry $\bar{d}/\bar{u}$ of the quark sea in the nucleon. Previous measurements through the Gottfried sum rule in DIS and Drell-Yan production in p+p scattering have relied on combining data from proton and deuteron targets assuming charge symmetry, $u_p(x) = d_n(x)$, $d_p(x) = u_n(x)$, $\bar{u}_p(x) = \bar{d}_n(x)$ and $\bar{d}_p(x) = \bar{u}_n(x)$, and assuming that nuclear effects are negligible. In W production $\bar{d}/\bar{u}$ can be obtained from the proton data alone, independent of assumptions about charge symmetry. Figure 21 compares calculations for the W cross section ratio R for four different sets of parton distribution functions with errors projected for the integrated run 12 + run 13 luminosity of $300\,\mathrm{pb}^{-1}$. The PDF set MRS-SO assumes a symmetric quark sea, $\bar{d}(x) = \bar{u}(x)$, and can be well separated within the projected experimental uncertainties from PDF sets that include the breaking of the quark sea. A detailed discussion of this measurement can be found in [37].

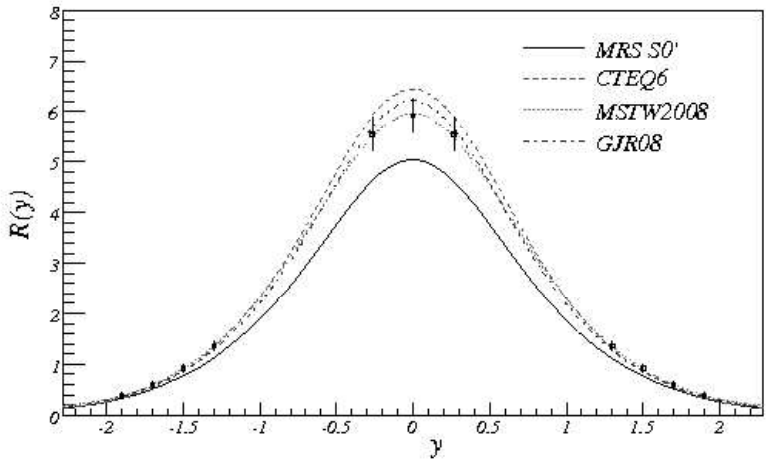

Figure 21: The ratio, R, of cross sections for W^+ and W^- production at $\sqrt{s} = 500\,\text{GeV}$ plotted versus the rapidity of the decay lepton. The projected errors represent the combined run 2012 and 2013 integrated luminosity of $300\,\text{pb}^{-1}$ into the PHENIX central and muon arms. The curves represent calculations of R for different PDF sets. The PDF set MRS-SO assumes a symmetric quark sea whereas the other PDF sets are based on asymmetric quark seas. The projections are from reference [37] and have been performed at the event generator level.

5.1.7 Measuring $\Delta G(x)$ in the range of $0.01 < x < 0.3$ (HP12,2013)

In PHENIX $A_{LL}^{\pi^0}$ is a well established tool for constraining the gluon contribution to the proton. As is shown on the right hand side in Figure 22, $\sqrt{s} = 500\,\text{GeV}$ collisions provide access to a lower x range than at 200 GeV.

The left hand side of Figure 22 shows the expected uncertainties in $A_{LL}^{\pi^0}$ as a function of p_T at 500 GeV for the project run 12 integrated luminosity of 100 pb[1] with the standard ± 30 cm vertex and a polarization of 50%. The calculation is for π^0 measured in the PHENIX central arms. As there is considerable material thickness due to the vertex detector support structure beyond the ± 10 cm vertex region, the estimation is based on only 18 pb^{-1} within ± 10 cm.

We will also utilize double spin asymmetries measured for π^0s and electromagnetic clusters reconstructed in the Muon Piston Calorimeter (MPC). These forward measurements will increase the reach to smaller x. The experimental method of using back-to-back

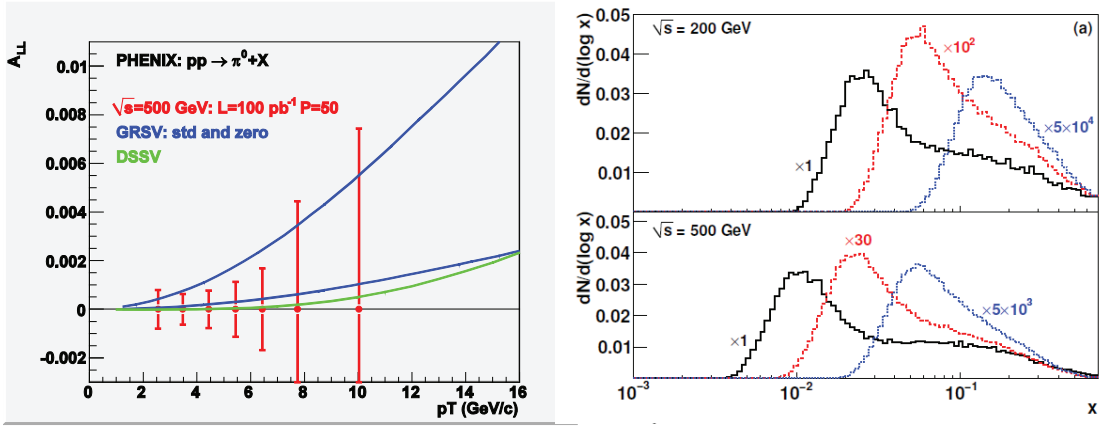

Figure 22: Expected uncertainties in $A_{LL}^{\pi^0}$ as a function of p_T in Run-12. Only collisions with vertex inside ± 10 cm are included. The projections are based on earlier measurements published by PHENIX.

hadron pairs in the MPC or one hadron in the MPC and a second in the central arm provides the ability to select different x_g depending on the choice of rapidities and transverse momenta of the hadrons. Di-hadron measurements have been successfully explored with the MPC for the 2008 d+Au and p+p data samples.The results have been submitted for publication recently [12]. In order to demonstrate the sensitivity of these measurements the double spin asymmetry, A_{LL}^{cluster} is shown in figure 23 together with the x_g distribution for this channel. The projected errors are for $\int Ldt = 300\,\text{pb}^{-1}$ and $P = 0.55$. The asymmetries shown have been obtained by setting $\Delta G(x)$ to DSSV-min in the simulations. At a $p_T = 1.5\,\text{GeV}$ the asymmetries are 2×10^{-4} rising to about 1×10^{-3} at $p_T = 6$ GeV. In order to fully exploit the sensitivity for $\Delta G(x)$ at small x_g it will be necessary to improve the uncertainty in the relative luminosity to below 10^{-4}.

5.1.8 Transverse Spin Physics

In addition to the dedicated p+p running at $\sqrt{s} = 500\,\text{GeV}$ for the nucleon spin program, $\int Ldt = 33\,\text{pb}^{-1}$ with $P = 0.6$ of p+p data at $\sqrt{s} = 200\,\text{GeV}$ will be taken in runs 12 and 13. This request is driven primarily by the heavy ion program requirements for p+p reference data. However, this presents a good overlap with the luminosity needs for

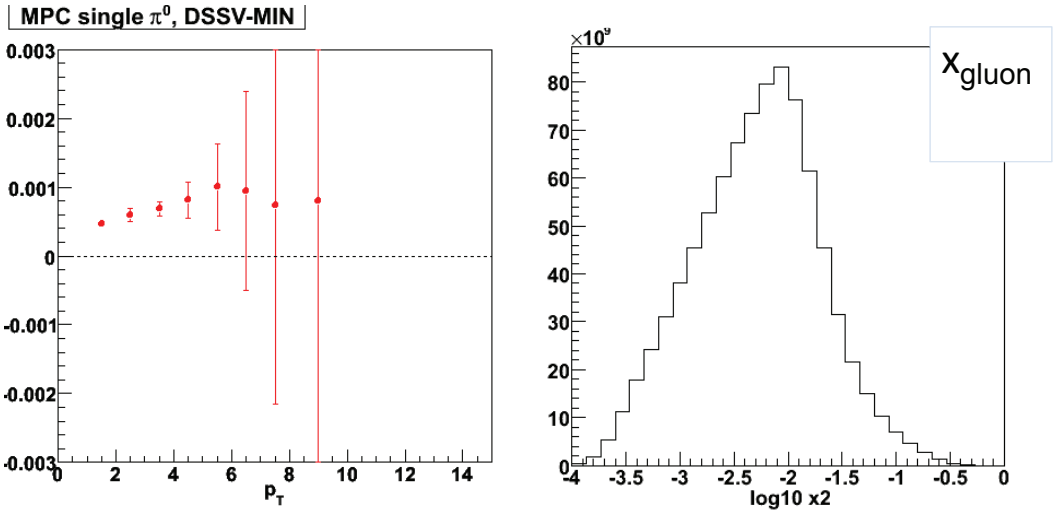

Figure 23: Expected uncertainties in the MPC cluster A_{LL} as a function of p_T for $\int Ldt = 300\,\mathrm{pb}^{-1}$ and $P = 0.55$. The asymmetries have been obtained by setting $\Delta G(x)$ to DSSV-min in the simulations. Also shown is the x_g distribution for this channel.

the transverse physics program in PHENIX. Currently the total recorded luminosity with transverse polarization is $8\,\mathrm{pb}^{-1}$ at $\sqrt{s} = 200\,\mathrm{GeV}$ with a beam polarization of $P = 0.5$ in 2006 and $P = 0.45$ in run 2008.

The proposed transverse running will make it possible to pursue currently marginal measurements with much improved statistical significance.First, the high p_T behavior of the original single spin asymmetries for inclusive hadrons at forward rapidity has still not been explained quantitatively. The precision of present data seems insufficient to guide theory at high p_T. It is important to carry out high statistics measurements of A_N at forward rapidities to characterize the p_T-dependence of A_N at forward rapidity and large p_T. Figure 24 shows projections of A_N for electromagnetic clusters (mostly π^0s) in the MPC.It will be possible to measure the p_T dependence of A_N with good precision up to a $p_T = 6$ GeV and to differentiate between different theoretical possibilities.

Secondly, it is generally assumed that A_N arises from multiple mechanisms, the Sivers effect in the initial state, the Collins effect in the final state and dynamic quark-gluon correlations at higher twist in the Operator Product Expansion (OPE). With the proposed luminosity it becomes possible to carry out measurements that isolate and directly probe the Collins and Sivers effects. We will discuss three examples for the data samples to be taken during runs 12 and 13: A_N in back-to-back hadron correlations probing the Sivers

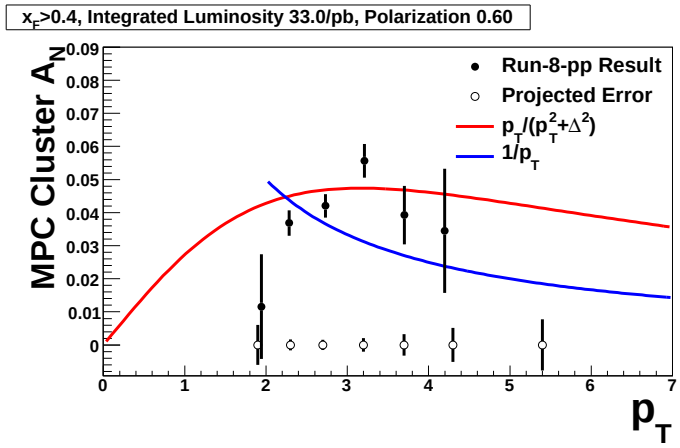

Figure 24: Previous results and expected uncertainties for $A_N^{cluster}$ as a function of p_T in Run-12.The projections are based on earlier measurements of A_N for electromagnetic clusters in the MPC. The blue curve represents the expected p_T-dependence at subleading twist, $A_N \sim 1/p_T$ and the red curve represents a simple model for re-summed contributions to A_N at all (odd) orders in the twist expansion.

mechanism, A_T in di-hadron interference fragmentation sensitive to quark transversity distributions and the measurement of Collins asymmetries in jets, probing again quark transversity distributions.

Probing Quark Transversity Distributions

Feng Yuan has proposed to measure the Collins effect at RHIC in jets. Ideally the measurement would consist of reconstructing jet axis and jet energy and then, as function of the fractional hadron momentum z, the measurement of the Collins asymmetry in the azimuthal distribution of the hadron around the jet axis with respect to the proton spin vector component normal to the plane defined by jet axis and beam momenta. In absence of full jet reconstruction capabilities the measurement is carried out in PHENIX by starting with a high p_T trigger particle in the central arms. After adding additional hadrons present close to the trigger particle a "quasi" jet axis is determined and the Collins asymmetry is then observed for hadrons on the away side with respect to the jet axis. The measurement has been studied by introducing transverse spin processes in PYTHIA. The Collins function is taken from the analysis of SIDIS and Belle data. The transversity distributions are tuned so that the simulations reproduce the cluster A_N measured in the MPC correctly. Two different assumptions are used. First it is assumed that 25% of the experimental A_N originates from the Collins effect. This assumptions corresponds to the Collins

asymmetry shown as dashed line in Figure 25. Alternatively, it is assumed that 100% of A_N results from the Collins effect. This assumption results in the solid line in Figure 25. The error bars in Figure 25 indicate the statistical sensitivity for $\int Ldt = 33\,\mathrm{pb}^{-1}$. With the statistics available from run 12 and 13 the measurement can directly rule out maximal Collins contributions to the inclusive transverse spin asymmetries A_N observed in p+p collisions.

The theoretical analysis of the Collins results his limited by the fact that factorization for transverse momentum dependent fragmentation functions (such as the Collins function) and parton distributions (such as un-integrated quark transversity distributions) may not hold for p+p collisions. It would be highly interesting to quantify the magnitude of the factorization breaking in p+p collisions. This may become feasible by comparing the results of an extraction of quark transversity distribution from Collins asymmetries in jets with an extraction based on the co-linear di-hadron interference fragmentation function (IFF), as factorization holds for. Significant differences between the extracted transversity distributions would indicate large effects in factorization and universality between SIDIS, e^+e and p+p.

PHENIX already has carried out an exploratory measurement of transverse spin asymmetries in di-hadron interference fragmentation. The results for $\int Ldt = 8\,\mathrm{pb}^{-1}$ are shown in Figure 26 together with projected errors for the run 12 and 13 measurement with Figure 25. A simple model based on quark transversity distributions extracted from SIDIS and Belle Collins asymmetries in combination with the most recent Belle result on interference fragmentation leads to the estimate that $A_T \sim 0.005$ in di-hadron fragmentation. This asymmetry can be easily detected in run 12 and 13 as the projections in Figure 26 show.

The extraction of quark transversity distributions from Collins and IFF asymmetries rests on the availability of independent information on the spin dependent fragmentation functions from e^+e^- annihilation. For this purpose, a group of PHENIX and STAR experimenters have joined the Belle collaboration and have successfully measured initially Collins- and recently IFF-asymmetries in jet fragmentation. The timely information from Belle will allow our theory colleagues to promptly analyze run 12 and 13 PHENIX data on Collins and IFF spin asymmetries and to extract quark transversity distributions probing for differences between the transverse momentum dependent Collins extraction and the co-linear IFF extraction of transversity quark distributions.

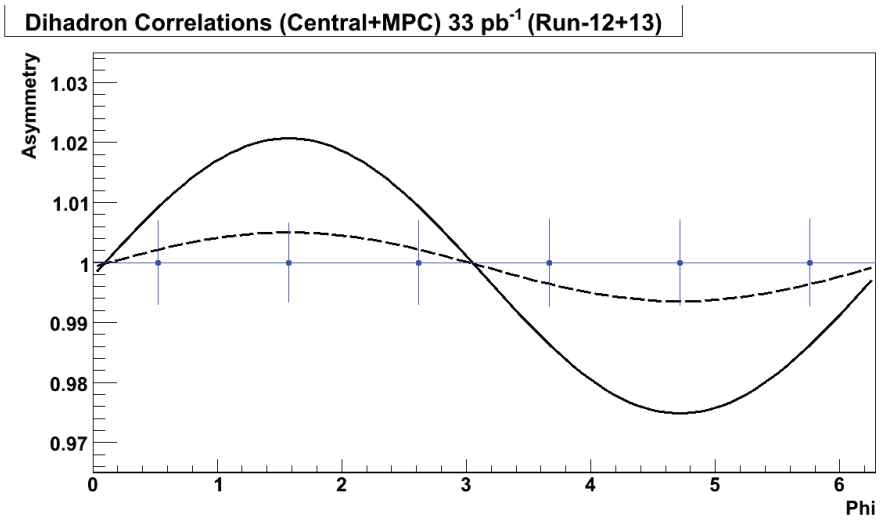

Figure 25: Projected uncertainties for Collins asymmetries in PHENIX. The projections are based on PYTHIA simulations tuned to reproduce the A_N measured in the MPC.

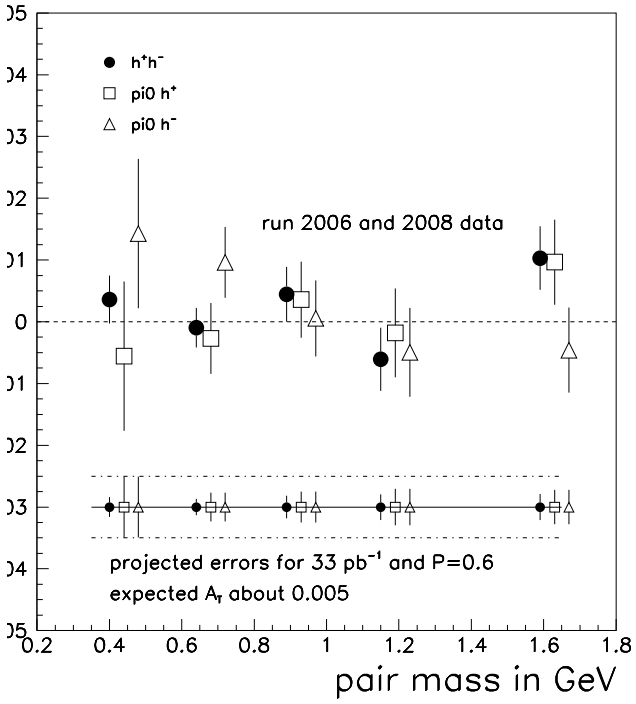

Figure 26: Previous results for the transverse spin asymmetry A_T observed in di-hadron interference fragmentation with the PHENIX central spectrometer arms and projections for run 12 and 13 measurement. A_T is shown for three different combination of hadron pairs. The projections for run 12 and 13 with $\int Ldt = 33\text{pb}^{-1}$ are based on earlier PHENIX results shown on the figure.

Probing Sivers asymmetries The integrated luminosity from runs 12 and 13 with transverse spin will also lead to better statistical precision in the A_N measurement of back-to-back hadrons. This measurement is sensitive to the presence of transverse momenta in the initial state and probes the Sivers effect. A comparison between previous results and projections for run 12 and 13 are shown in Figure 26.

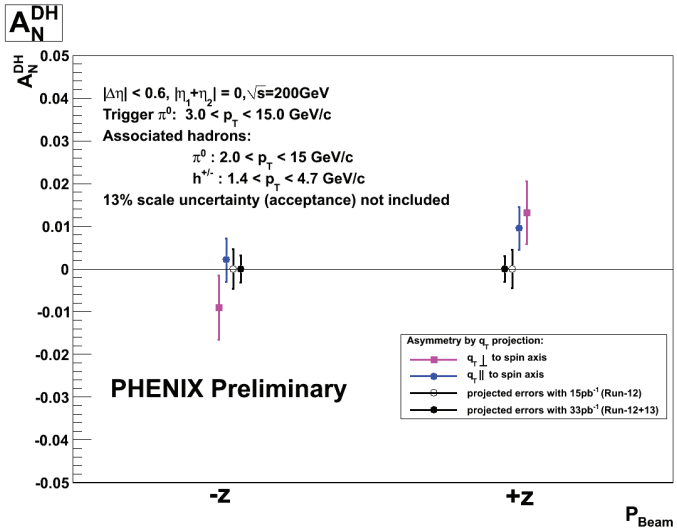

Figure 27: Previous results and expected uncertainties for A_N for back-to-back hadrons for $\int Ldt = 33\,\mathrm{pb}^{-1}$ in runs 12 and 13.The projections are based on earlier measurements of A_N for back-to-back hadrons in PHENIX.

5.1.9 200 GeV Au+Au collisions

PHENIX has exceptional electron particle identification, even in the high multiplicity environment of central Au+Au reactions. PHENIX has published [2] Au+Au results from the 2004 run on nonphotonic electrons, which are predominantly from charm and bottom meson decays. Figure 28 shows the measurements of the nuclear modification factor R_{AA} out to $p_T \approx 10\,\mathrm{GeV}/c$ and elliptic flow v_2, which indicate a dramatic change in the momentum distribution of heavy quarks in the medium. If the heavy quarks were unaffected by the surrounding Quark Gluon Plasma, the R_{AA} value would be close to one (excepting modest initial state effects) and v_2 would be zero. This Letter has been cited 200 times in the last three years which is a simple indicator of the strong interest in the field in these results. In a recent manuscript submission we have extensively documented

the entire analysis procedure for nonphotonic electrons, including systematic uncertainty estimation, and theoretical model comparisons [9].

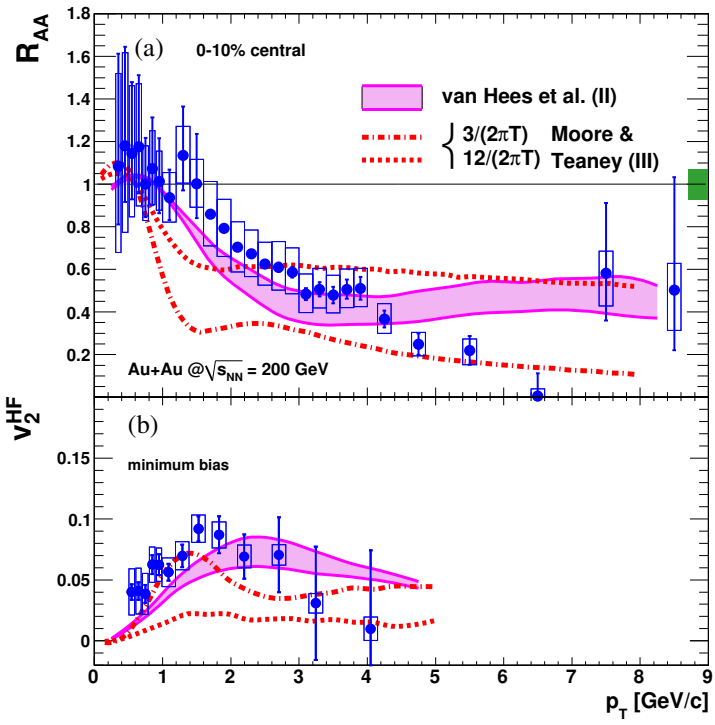

Figure 28: (a) Nuclear modification factor R_{AA} of heavy-flavor electrons in 0–10% central collisions compared with PHENIX π^0 data and various model calculations. The box at $R_{\mathrm{AA}} = 1$ shows the uncertainty in the number of binary collision estimate. (b) v_2 of heavy-flavor electrons in minimum bias collisions compared with PHENIX π^0 data and the same models.

As shown in Figure 29, these results present a challenge for the perturbative (weak coupled expansion approximation) picture of partonic energy loss. However, a fundamental complication is that the nonphotonic electrons have contributions from both charm hadron (e.g. D meson) and bottom hadron (e.g. B meson) decays. It is expected that charm hadrons dominate the electron contribution for $p_T < 5\,\mathrm{GeV}/c$ and bottom hadrons for $p_T > 5\,\mathrm{GeV}/c$. This is roughly confirmed by examining nonphotonic electron-hadron angular correlations in p+p reactions [5]. However, the statistical uncertainties are large and the current perturbative QCD FONNL calculations have an uncertainty in the ratio of $b \to e/c \to e$ ratio from approximately 0.3 to 0.7 at $p_T = 5\,\mathrm{GeV}/c$.

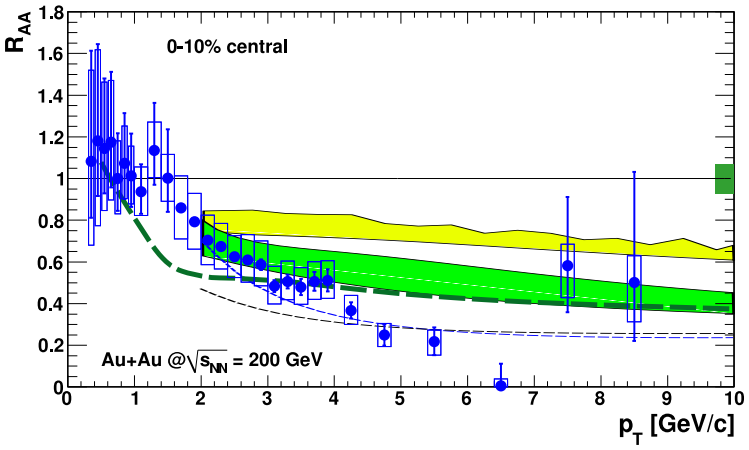

Figure 29: R_{AA} in the 0–10% centrality class compared with energy loss models. The thick dashed curve is the BDMPS calculation for electrons from D and B decays. The bands are DGLV calculations for electrons from D and B decays. The lower band contains collisional energy loss as well as radiative energy loss. The thin dashed curves are DGLV calculations for electrons from D decays only.

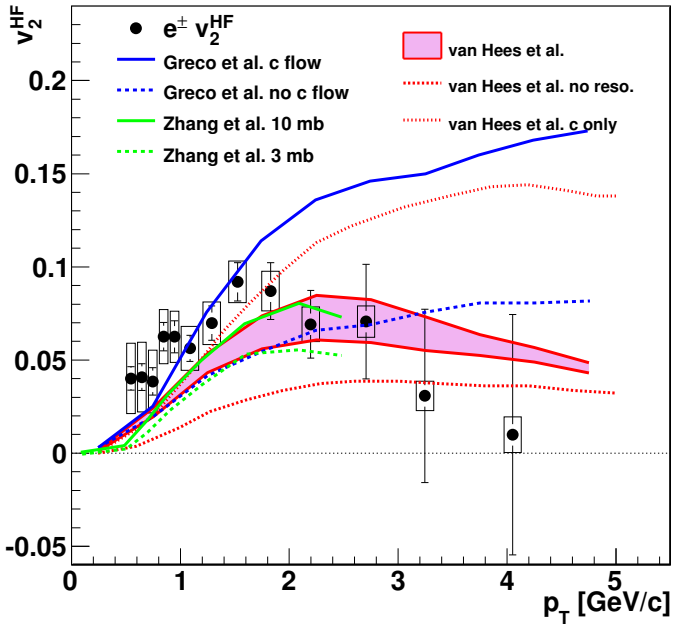

Figure 30: Nonphotonic electron (HF) elliptic flow (v_2) as a function of transverse momentum compared with theoretical models from Greco *et al.*, Zhang *et al.*, and van Hees *et al.*

Figure 30 shows a number of calculations of charm quark flow in the Quark Gluon Plasma. At $p_T = 5$ GeV/c, some calculations of v_2 range as high as 15%. The data do not support a monotonic increase of v_2 with p_T, despite large statistical uncertainties. The trend seen in the data could be the result of reduced charm quark flow, or it could be due to a predominance of bottom quark contributions at higher p_T.

Diffusion calculations show that bottom quarks are so heavy that they are difficult to move around, and thus exhibit minimal flow. In the perturbative energy loss framework, radiative energy loss of heavy quarks via gluon bremsstrahlung is suppressed due to the "dead cone" effect, where forward radiation for heavy quarks, traveling at velocities much less than the speed of light, is limited. If, contrary to expectations, the bottom quarks exhibit strong flow in the medium, this would challenge the entire paradigm of perturbative energy loss as the proper framework for understanding jet quenching. Additionally, a measurement of charm flow (separated from bottom flow) out to higher p_T may well provide one of the best constraints on the η/s ratio via the diffusion approach. This method for constraining η/s is an excellent alternative to the current method which compares the bulk flow of light hadrons to viscous hydrodynamic models. It would help us answer the question of how close η/s in the quark-gluon plasma is to the conjectured minimum bound.

The VTX was installed on schedule in the fall of 2010, and will be followed by the installation of the FVTX in the fall of 2011. The first Au+Au run with the capability of measuring displaced vertices of leptons from the decay of charm and bottom mesons is currently underway, utilizing the VTX. We are currently acquiring physics data with the detector in its initial Au+Au run. However, additional running is needed to exploit the VTX and achieve the uncertainties shown below. Run-12 will allow commissioning of the FVTX in both p+p and Au+Au events, however full utilization of the FVTX will certainly require additional Au+Au running beyond Run-12. For comparison $p+p$ measurements at 200 GeV, we require an integrated luminosity over two years of running of 15 pb^{-1} sampled within the same z-vertex acceptance.

We also anticipate a longer run when full accelerator stochastic cooling becomes available, and additional data acquisition bandwidth via the SuperDAQ upgrade is installed. In total this will yield 4.3 (3.6) nb^{-1} or equivalently 29 (24) billion recorded Au+Au interactions for the VTX (FVTX). All of these event number projections take into account the smaller z-vertex acceptance (i.e., $\pm$10 cm) of the silicon detectors. We show the projected physics performance we expect to achieve by 2015, using the above integrated luminosities over multiple year running periods. Shown in Figure 31 is the nuclear modification

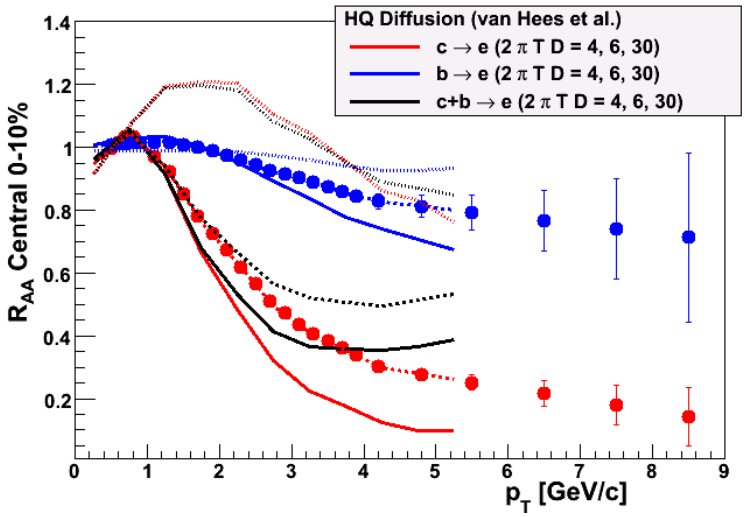

Figure 31: Projected uncertainties for the nuclear modification factor ($R_{\rm AA}$) as a function of transverse momentum for heavy flavor electrons tagged with a displaced vertex from D meson decay (red) and B meson decay (blue). The uncertainties are for the 10% most central Au+Au collisions—a subset of a total of 29 billion Au+Au minimum bias events and 14.8 pb^{-1} p+p events at 200 GeV. Also shown are calculations by van Hees *et al.* [33] assuming different diffusion coefficients.

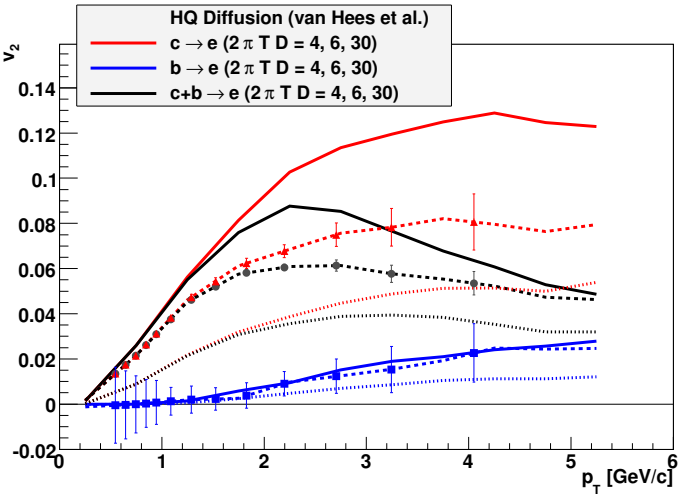

Figure 32: Shown are the projected uncertainties for the elliptical flow (v_2) as a function of transverse momentum for heavy flavor electrons tagged with a displaced vertex from charm hadron decay (red) and bottom hadron decay (blue) and the combination of the two (black). The uncertainties are for 10% central Au+Au reaction as a subset of a total of 29.0 billion Au+Au minimum bias events as projected to be accumulated by 2015. Also shown are calculations from van Hees *et al.* [33] in a heavy quark diffusion calculations assuming different diffusion coefficients. Note that the largest flow magnitude case corresponds to nearly zero shear viscosity.

factor R_{AA} of electrons from charm and bottom hadron decays. Figure 32 shows the projected uncertainties for minimum bias Au+Au collisions for the elliptic flow v_2 observables. For the elliptic flow projections, we have assumed a reaction plane resolution comparable to that from the reaction plane detector that was installed prior to 2007. This detector was removed after the 2010 running period due to conflicting space requirements with the VTX, but studies indicate that the VTX and FVTX can be similarly utilized with a comparable resolution. These results will provide great insight into the puzzles of the behavior and interaction of heavy flavor quarks in the medium.

The FVTX provides an excellent opportunity to measure the open heavy flavor suppression and flow at forward rapidity. Here the measurement is also sensitive to low-x gluons in the gold nucleus, and will provide a baseline measurement for comparison with the J/ψ suppression seen in the same kinematic range. Shown in Figure 33 are the projected

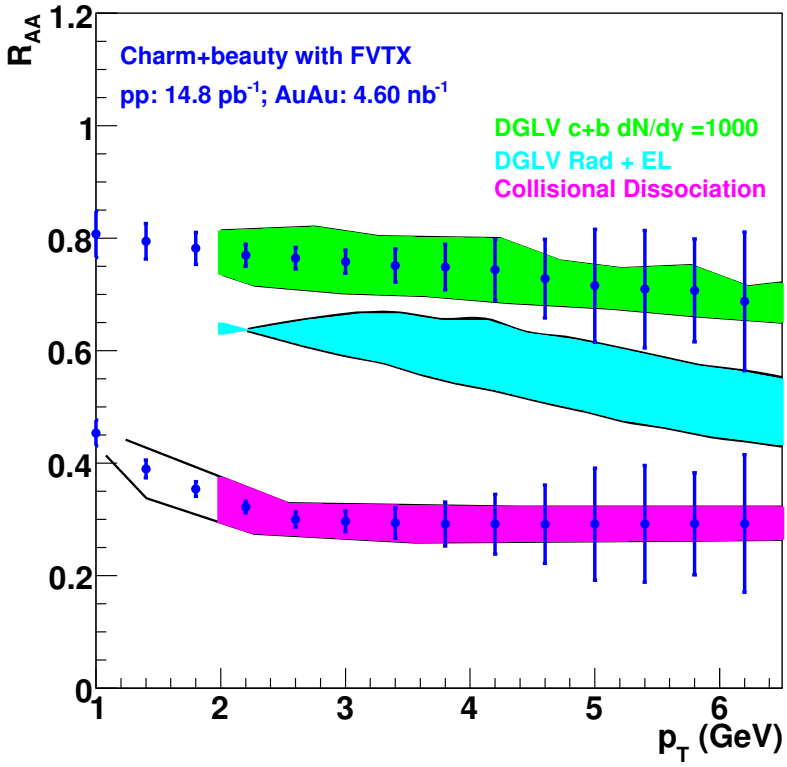

Figure 33: Projected heavy flavor $R_{\rm AA}$ measurement with the FVTX versus transverse momentum p_T, compared with three different theoretical expectations.

measurement uncertainties on $R_{\rm AA}$ for heavy flavors, using muons that are tagged by the FVTX as originating from heavy meson decays. This displays a very clear discriminating power between different energy loss scenarios: 'DGLV' including perturbatively calculated radiative energy loss only [24], 'DGLV Rad + El' which includes additional elastic energy loss [35], and collisional dissociation of the mesonic state in the medium [13]. These measurements will provide excellent discriminating power between these different scenarios.

Collecting an identified open heavy flavor data set for p+p, d+Au and Au+Au that covers a broad rapidity range address the following physics topics:

- The determination of the rapidity, centrality, and p_T dependence of the modification of open heavy flavor from the combined p+p and d+Au data (p+p in Run-13, d+Au most logically in Run-14). This will provide an excellent data set that will address the behavior of gluon modification vs nuclear density. Open heavy flavor has the advantage over J/ψ measurements that it is not subject to modification by collisions with nucleons during the heavy ion collision, and so avoids the complication that arises for J/ψ production, where a breakup cross section must also be determined from the data. There is little theoretical guidance for the J/ψ breakup cross section, and it possibly has a significant dependence on rapidity.
- Once the role of cold nuclear matter effects is quantified in p+p and d+Au data, the contributions to Au+Au collisions can be predicted, and the effects of hot nuclear matter on the open c and b cross sections can be isolated using the Run-13 Au+Au data set. This will permit the study of energy loss of heavy quarks in hot nuclear matter over a broad rapidity range.

In addition to its critical role in studying gluon modification vs nuclear density at low x, and isolating hot nuclear matter effects over a broad rapidity range, the FVTX will make important improvements in the quarkonium measurement capabilities at forward and backward rapidities by improving the mass resolution and improving the signal to background for quarkonium measurements. This is particularly important for studying $\psi\prime$ cold and hot nuclear matter effects using p+p, d+Au and Au+Au collisions.

The p+p and Au+Au data sets will be obtained in Run-12 and Run-13, with a possible continuation into Run-14. The d+Au data set would become a high priority for Run-14.

What answers can we expect with an 8 week Au+Au run at 200 GeV? At this time, CAD projects a peak luminosity of $40 \times 10^{26} cm^{-2} s^{-1}$ and an average store luminosity of $20 \times 10^{26} cm^{-2} s^{-1}$. The VTX detector spans a range along the beam axis from -10.0 cm to +10.0 cm. Thus, collisions that occur outside this narrow region will produce particles that have a much smaller acceptance for hits in the VTX, in addition to encountering almost a full one radiation length of material (the support structure and readout for the VTX). The fraction of all collisions expected within this narrower z-vertex range is approximately 25%. This was achieved in Run-10 and is matched in Run-11 at the time of this writing.

In Run-10, the PHENIX Data Acquisition system was able to record 5 kHz of minimum bias Au+Au events. The VTX detector installation is also coupled with new data acquisition electronics (the Data Collection Module II) and upgrading the Event Builder switch (as part of the PHENIX DAQ/Trigger 2010 project). The upgrades for reading out the VTX have full capabilities in significant excess of 5 kHz, and this has now been demonstrated in Run-11. However, this will be the first running period for the FVTX, which will require commissioning time and periods with rates below the ultimate performance specifications. Thus, we assume an average data taking rate of 2.5 kHz during this running period (with the possibility for improved performance during the run). At this rate, we are limited by the beam luminosity during the first few weeks of ramp-up, and data acquisition rate limited thereafter (assuming only the 2.5 kHz rate). Thus, we estimate that after 2 weeks of setup and for 7 weeks of physics data taking, we would record at least 4.7 billion minimum bias Au+Au events at full energy.

It is important to note that the full measurement is a multi-year program. Utilizing the data from one run, the error bars on Figures 31 and 32 will be larger by a factor of about $\sqrt{6}$. This implies central rapidity measurement by the VTX of b quark R_{AA} to 6 GeV/c p_T and v_2 to approximately 3 GeV/c. Combining two data sets will reduce the error bars by a factor of $\sqrt{2}$, increasing the p_T reach accordingly. Similar factors in the error bars apply for measurements with the FVTX. PHENIX considers it vital to begin this program immediately, also in the forward region, in order to utilize our new detectors and to be competitive with heavy flavor measurements at the LHC.

5.1.10 U+U at $\sqrt{s} = 193$ GeV

One of the unique capabilities of RHIC, in contrast to the LHC heavy ion program, is its capability to deliver large data sets changing the geometry using U+U collisions as well

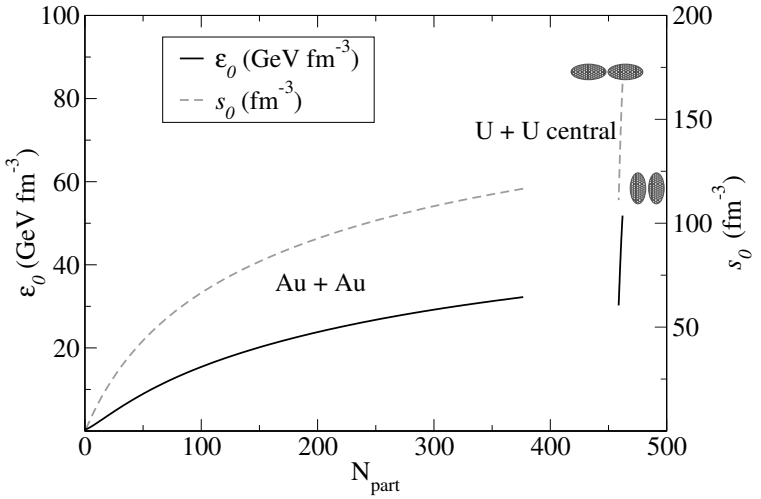

Figure 34: Energy density and entropy density as a function of the number of participating nucleons for Au+Au and U+U collisions (from [26]).

as asymmetric beam species. This gives the possibility of varying the eccentricity for the study of anisotropic flow and the path length for the study of parton suppression. When comparing to theoretical models, such studies should be sensitive to early time dynamics and thermalization. The PHENIX run plan includes two such systems—U+U collisions made possible by EBIS and Cu+Au collisions.

There is significant anticipation for the availability of Uranium beams at RHIC. The key physics interest arises from the significant deformation of Uranium nuclei (non-sphericity). Figure 34 shows calculations indicating that in tip-tip collisions (as illustrated) a higher energy density is achieved. Probing this higher energy density can provide key tests of hydrodynamic behavior and the path-length dependence of parton energy loss [26]. More recently, it has been proposed [34] that body-body collisions (as illustrated in Figure 1) may be an excellent test of the hypothesized local parity violating bubbles. These collisions near impact parameter $b = 0$ should have zero magnetic field and thus no charge separation effect related to local parity violation, while the overall eccentricity remains large (thus allowing one to examine competing flow and fluctuations effects). The key to utilizing Uranium collisions for these purposes is the ability to disentangle the various geometries of the individual interactions. For two spherical nuclei, one impact parameter value (b) determines the initial nuclear geometry (and then fluctuations of the nucleon positions within each nuclei). However, in U+U collisions, in addition to the impact parameter, the two nuclei have rotations in spherical coordinates($\theta_1, \phi_1, \theta_2, \phi_2$). Numerous papers have made proposals for separating these various geometries [28, 30, 31, 25].

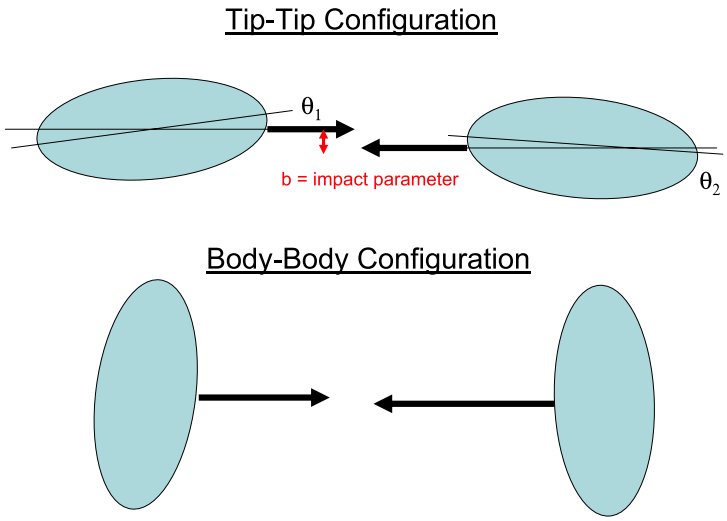

Figure 35: Uranium-Uranium geometry picture showing the tip-tip configuration (upper) and the body-body configuration (lower).

In order to study and reproduce some of these proposed methods, we have modified the PHOBOS Glauber Monte Carlo [17] to include the uranium geometry following the prescription in [28] and also the forward neutron distribution (for modeling the response in the Zero Degree Calorimeters). If the charged particle multiplicity $dN_{ch}/d\eta$ at mid-rapidity is correctly described by the two-component model (as discussed in [25]) where:

$$\frac{dN_{ch}}{d\eta} \propto (1 - X_{hard}) \times \frac{N_{part}}{2} + X_{hard} \times N_{binary} \tag{3}$$

then the very highest multiplicity events can simply be selected with a highly enhanced tip-tip contribution. However, the two-component model yields 10% discrepancies when comparing Au+Au to Cu+Cu reactions and alternative scalings have also been successful. It is notable that in [29] they discuss Uranium geometries in terms of gluon saturation effects and find a smaller selectability in these highest multiplicity events. An initial data sample is necessary in order to test these various pictures (which is of physics interest in its own right), to then understand how the geometry can be disentangled. The selectivity within the two-component model alone and a cut on charged particle multiplicity for the top 0.2% and 0.04% is shown in Figure 36. The angular selection for the tip-tip configuration remains rather broad.

Additional proposals have been made that one can select event categories by a combination of elliptic flow and multiplicity or zero degree energy. For tip-tip collisions, the

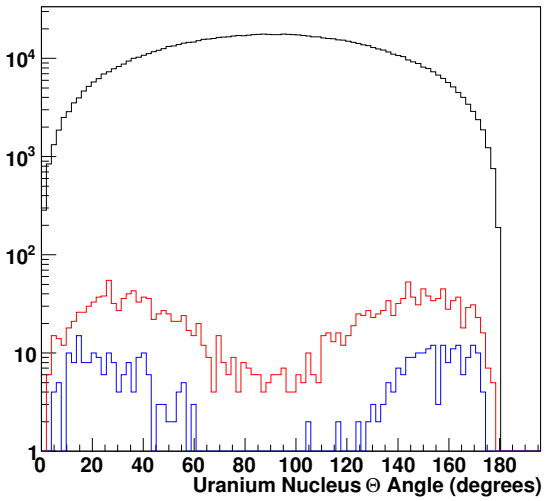

Figure 36: Glauber Monte Carlo results for Uranium-Uranium collisions for the θ angle of one nucleus. The black histogram is all collisions (i.e. random geometry), the red curve is selecting the highest 0.2% based on charged particle multiplicity (assuming the two-component model) and the blue curve is selecting the highest 0.04%.

eccentricity is small and thus the elliptic flow (v_2) should be small. However, this becomes quite complicated for some of the physics goals (for example testing the limits of the hydrodynamical models) because one has used a specific observable of interest to hydrodynamics in the event selection; this can produce a bias. Alternatively, body-body collisions might be selected by looking for almost no zero degree energy and then large eccentricity via large v_2. However, PHENIX finds that even in the most central Au+Au reactions, there is still non-zero energy in the zero degree calorimeters. This is likely due to a few percent probability to have the nucleons interact, but charge exchange a proton to a neutron or have a very small angle scatter of the initial neutron.

Shown in Figure 37 (left panel) is the modeled distribution for charged particle multiplicity (based on the two-component model) versus the zero degree energy. We select the $dN_{charge}/d\eta > 700$ and $ZDC_{energy} < 1500\,GeV$ (corresponding to 0.6% of the total cross section), and find that almost all such events have impact parameter $b < 2$ fm.

In Figure 37 (right panel) we show the participant eccentricity (ϵ_{part}) distribution for these events. In black are the events aligned within 30 degrees of tip-tip (and one can see the preference for small eccentricity) and in red are the events aligned within 30 degrees of

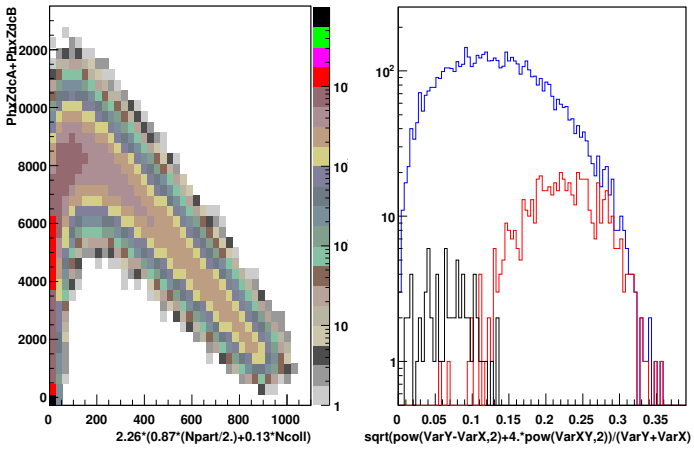

Figure 37: Shown in the left panel is the modeled distribution for charged particle multiplicity (based on the two-component model) versus the zero degree energy. In the right panel we have selected the smallest 0.6% impact parameter events based on the left panel distribution and we show the participant eccentricity (ϵ_{part}) distribution for these events. In black are the events aligned within 30 degrees of tip-tip (and one can see the preference for small eccentricity) and in red are the events aligned within 30 degrees of body-body (and one can see the preference for larger eccentricity and for $\epsilon_{part} > 0.25$ this dominates the sample).

body-body (the preference for larger eccentricity and for $\epsilon_{part} > 0.25$ this dominates the sample). There are many model assumptions that go into this calculation that need validation with real data, but the results show promise. Consequently, the PHENIX Beam Use Proposal supports a modest commissioning run, with the possibility for longer running in the coming physics runs.

The Electron Beam Ion Source (EBIS) will provide a new heavy ion pre-injector for RHIC based on a high charge state heavy ion source, a Radio Frequency Quadrupole (RFQ) accelerator, and a short Linear Accelerator. EBIS has the potential for significant future intensity increases and can produce heavy ion beams of all species including uranium (that has been previously unavailable). In the most recent "RHIC Collider Projections (FY 2011–FY 2015)" dated May 11, 2010, the stated luminosity average for a store is $8 \times 10^{26} cm^{-2} s{-}1$ corresponding to an interaction rate of approximately 5.5 kHz. Since the β^* is quoted at 0.65 meters, we assume that 55% of collisions will take place within the z-vertex ($|z| < 30$ cm) and 30% within the z-vertex ($|z| < 10$ cm), corresponding to average interaction rates of 3.0 kHz and 1.6 kHz respectively. For most of the physics of

interest in a short Uranium-Uranium run, the full acceptance of the new silicon vertex detector (VTX) is necessary. Consequently, we will primarily focus on the narrowest z-vertex range. In the projections document, it states that at the end of the initial ramp-up period the luminosities may be "lower than at the end of the running period by a factor of 2-4" (where the above numbers were "after a sufficiently long running period."). Thus, for planning purposes, we will assume during a short initial commissioning run a factor of 3 lower rate, resulting in 530 Hz of U+U interactions within $|z| < 30$ cm.

In a period with 0.5 weeks setup for U+U (after full energy Au+Au running) followed by 1.5 weeks of data taking, PHENIX can record $\mathbf{150 - 200}$ million minimum bias U+U interactions. A 200 million event data sample would yield approximately 400,000 events in the tip-tip configuration, corresponding to approximately 0.2% of the cross section. This should be sufficient for geometry studies. Note that if one could perfectly select events with impact parameter $b < 2$ fm and with both nuclei aligned within less than 30 degrees of the tip-tip configuration, this corresponds to only 0.03% of the total cross section. Given the rate estimates for this commissioning run, measurements for these configurations involving rare probes or high p_T will not be possible.

Based upon these considerations, we request $0.5 + 1.5$ weeks for commissioning the uranium beam collisions and followed by collection of the data samples necessary to study the various geometry issues in Run-12.

For Run-13, we request a 5 week run yielding a useful integrated luminosity of 0.57/nb which will yield about 4 billion minimum bias U+U events or an event sample similar to that which would be collected Au+Au collisions in Run-12, with its complement of physics signatures. This would give us about 8M events in the tip to tip configuration or a sample similar to the central events obtained in the Run-2 Au+Au run, i.e. enough to begin doing rare probe physics in the tip to tip configuration.

5.1.11 Energy Scan

PHENIX requested 1 week of Au+Au collisions at 27 GeV for Run-11. The goal was to measure v_2 for identified hadrons and R_{AA} of π^0. As this run did not take place in Run-11, we request it in Run-12. We will measure not only v_2, but also v_3, and utilize the combination to measure the viscosity to entropy ratio η/s by comparison to viscous hydrodynamics calculations. We will search for the breaking of constituent quark scaling

of flow, and for the onset point of pion suppression.

In order to fully utilize the Au+Au energy scan data collected at 62 and 39 GeV in Run-10, we request p+p collisions for comparison at the same energies. Although the 62 GeV run was initially motivated by open heavy flavor and dileptons with the HBD, the excellent performance of RHIC allowed PHENIX to measure J/ψ production at both 62 and 39 GeV. The results were quite surprising. As can be seen in Figure 7, the J/psi suppression observed at 62 GeV is very similar to that at 200 GeV; suppression at 39 GeV is also consistent, though the statistical error is quite large. These results suggest that the similarity of $J/psiR_{AA}$ at top RHIC energy to that at top SPS energy cannot be due to

accidental cancellation of several different effects. However, quantitative comparison is not currently possible. Without sufficient p+p reference data at 62 GeV, we can only compare the ratio of

J/psi yields in central to peripheral collisions. The requested p+p reference data will allow us to report R_{AA} instead. A p+p reference data set at 39 GeV will allow calculation of a minimum bias R_{AA}; this will have smaller error bars than the current R_{cp}, which requires breaking the Au+Au data into two centrality bins.

Using the observed R_{AA} of 0.25 for 62.4 GeV Au+Au, and the fact that we collected $4.5\,\mathrm{pb}^{-1}$ p+p equivalent Au+Au collisions in Run-10, we estimate that $0.84\,\mathrm{pb}^{-1}$ of p+p reference data are necessary (this number also takes into account the higher efficiency for J/ψ reconstruction in p+p). The CA-D guidance states that the average luminosity for 62.4 GeV p+p collisions is $4.8 \times 10^{30} cm^{-2} sec{-}1$. This yields a daily rate of 0.124 pb^{-1} recorded by PHENIX with a vertex cut of $\pm$ 30 cm, appropriate for the muon arms. Consequently, we request one week of 62.4 GeV p+p to collect $0.84\,\mathrm{pb}^{-1}$.

At 39 GeV, CA-D advises that the luminosity is half as large, resulting in a daily rate of $0.062\,\mathrm{pb}^{-1}$ recorded. Our 39 GeV Au+Au data set from Run-10 is $1.6\,\mathrm{pb}^{-1}$ p+p equivalent. If we use a centrality-integrated R_{AA} of 0.6, and correct for relative reconstruction efficiencies, we estimate that $0.72\,\mathrm{pb}^{-1}$ of p+p reference data are needed. This would require 11.6 days, which does not fit into even the optimistic number of cryo weeks. In one week of data taking, we could record $0.434\,\mathrm{pb}^{-1}$ with a vertex cut of $\pm$ 30 cm.

5.2 Run-13

5.2.1 p+p in Run-13

As described above, the spin goals require combining multiple runs to gain the required statistical precision. Our highest priority for Run-13 is to continue collecting data on polarized p+p collisions at 500 GeV. Our request for 200 pb^{-1} in a vertex of $\pm$ 30 cm in Run-13, combined with the 100 pb^{-1} requested for Run-12, will allow us to achieve the performance shown in the Run-12 discussion above.

Our third priority for Run-13 is to record 20 pb^{-1} into $\pm$ 30 cm of 200 GeV transversely polarized p+p collisions. This will allow us to reach our transverse physics goal and provide comparison data for the FVTX. Should we not collect sufficient Au+Au data in Run-12 for physics with the FVTX, we will revisit and possibly re-prioritize this goal, along with the following heavy ion goals.

5.2.2 Cu+Au at $\sqrt{s} = 200\,\mathbf{GeV}$

Our second priority for Run-13 is to study Cu+Au collisions for the first time. We aim to record 2.4 nb^{-1} into a vertex cut of $\pm$ 10 cm.

The collision of asymmetric beams makes available two geometric situations not possible when colliding Au+Au or any other symmetric systems. First, for non-central collisions, the eccentricity of the collisions region does not have right left symmetry (Figure 38a) and can give rise to odd harmonics of flow from the geometry. (It is also possible to get such odd harmonics in symmetric collisions from eccentricity fluctuations[16].) Figure 38b illustrates this effect. Odd flow harmonics, in particular v_1 resulting from ϵ_1 and v_3 resulting from ϵ_3 should be measurable. ϵ_1 is significant at $N_{part} \sim 40$, which corresponds to an impact parameter of 9 fm. Since the radius of Au is about 7 fm and the radius of Cu is about 4.5 fm ($A = 63$), this corresponds to a geometry where the center of the Cu is at the outer edge of the Au nucleus. The rise in ϵ_1 at $N_{part} \approx 180$ corresponds to the case where the Cu nucleus is has just become fully contained in the Au nucleus with the outer edges lined up. Whether this will result in a measurable v_1 will be an interesting experimental question.

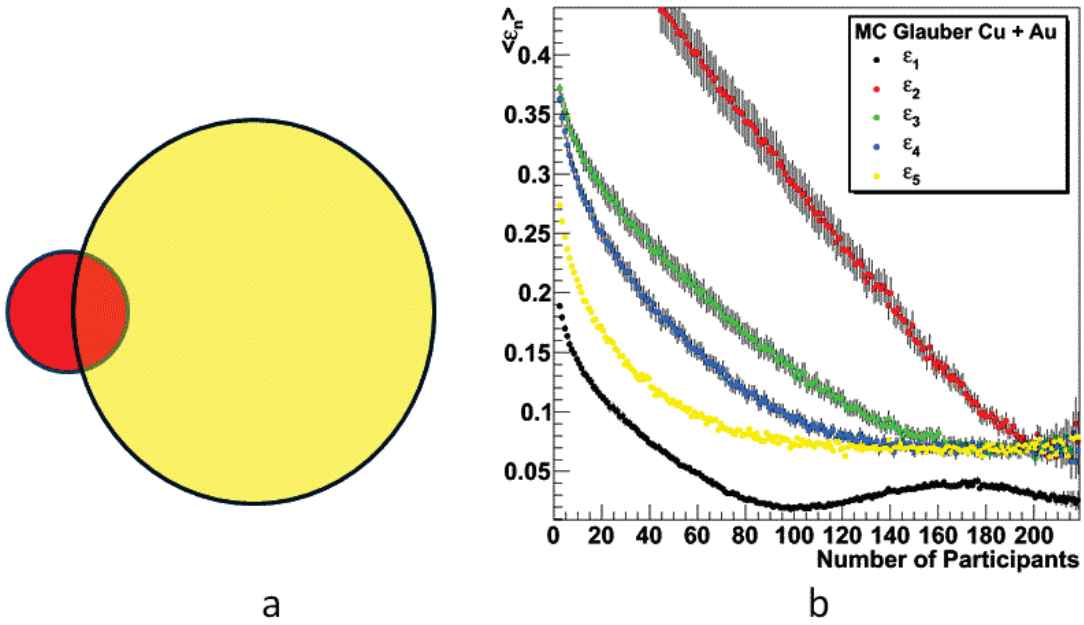

Figure 38: (a)A schematic of an exaggerated Cu+Au collision illustrating the collision region with left-right asymmetry. (b) ϵ_1 - ϵ_5 for Cu+Au collisions vs. the number of participants.

The measurement of flow in a variety of geometric configurations may be able to give information on early time dynamics and thermalization, for example via parton scattering cross sections[18]. Comparisons can be made between data from a variety of colliding systems and theory to yield physically meaningful parameters such as the viscosity or the thermalization time. Recently PHENIX has made a measurement of the elliptic flow of thermal photons. Such a signature, will be particularly useful when measured in Cu+Au and U+U collisions in elucidating information about the early stages of the sQGP.

Secondly for very central Cu+Au collisions, the Cu nucleus is essentially buried in the Au nucleus, giving a configuration in which the effect of the low density surface is minimized, since the Cu nucleus has interacted with the dense center of the Au nucleus. The interpretation of two particle correlations, and jet-jet correlations have been complicated by the fact that many jets, particularly those which are unquenched, may emerge because they are formed at the edge, in the low density region.

In Cu+Au collisions the low density surface region can be minimized by going to very central collisions. It has been suggested that the highest density region may be com-

pletely opaque, even for heavy quarks and as such partons from very central Cu+Au collision should not reach the surface. If the photon-jet signature is used, the photon would emerge, but the balancing quark or gluon would always be absorbed by the medium. It would also be possible to look at less central collisions, i.e. where the edges line up to introduce a small low density surface region. In this way the path length traversed by the outgoing quarks can be varied as done in symmetric systems. Interaction signatures such as the suppression of light quark jets, heavy quarks, and quarkonia can all be studied using this tool. Again, a comparison to Au+Au collisions and to theory should shed light on the energy loss in the medium, and possible quarkonium dissociation and/or recombination.

The geometry of Cu+Au collisions is much simpler than in U+U collisions since there is only one variable, the impact parameter. In addition the RHIC community has already had experience with asymmetric species when d+Au collisions were studied. For non-central collisions standard methods measuring spectator neutrons in the ZDC and the multiplicity in the BBC can be used. The case in which the Cu nucleus in completely contained within the Au nucleus is particularly interesting. Figure 39a shows the distribution of the number of participants from the Cu nucleus for minimum bias collisions. The enhancement of the contained case can be see at $N_{\rm part} > 60$ which accounts for about 3% of the cross section. If we take these events then plot the multiplicity (again assuming a two component model) vs. the impact parameter (Figure 39b), we can select those events which are preferentially very central, or those in which the Cu is contained in the Au nucleus but are less central. A cut on the multiplicity of between 360 and 380, yields events with an average impact parameter of about 0.8 fm. A cut of 320 to 340 yields events with an average impact parameter of about 1.5 fm—i.e., central events where the edges coincide (Figure 39c).

For run 13 we request a run of 5 weeks giving us a useful integrated luminosity of 2.4/nb or about 10 billion minimum bias events. As in the case of the U+U request, this will make accessible all physics signatures expected in a good Au+Au run. The top $\sim$3% (300 million events) of the cross section corresponds to those events where the Cu nucleus is contained in the Au nucleus. About 0.1% or 10 million events are those in which the Cu passes through the very center of the Au nucleus, with an average impact parameter of about 0.9 fm. (Note: the ratio between events within $b = 0.9$ fm and 1.5 fm does not go as the ratio of the areas because of the smearing effects between the multiplicity and the impact parameter.) This is enough to begin to look at rare probes such as charm and J/ψ suppression in very central events as compared to less central, where the Cu nucleus is still within the Au nucleus.

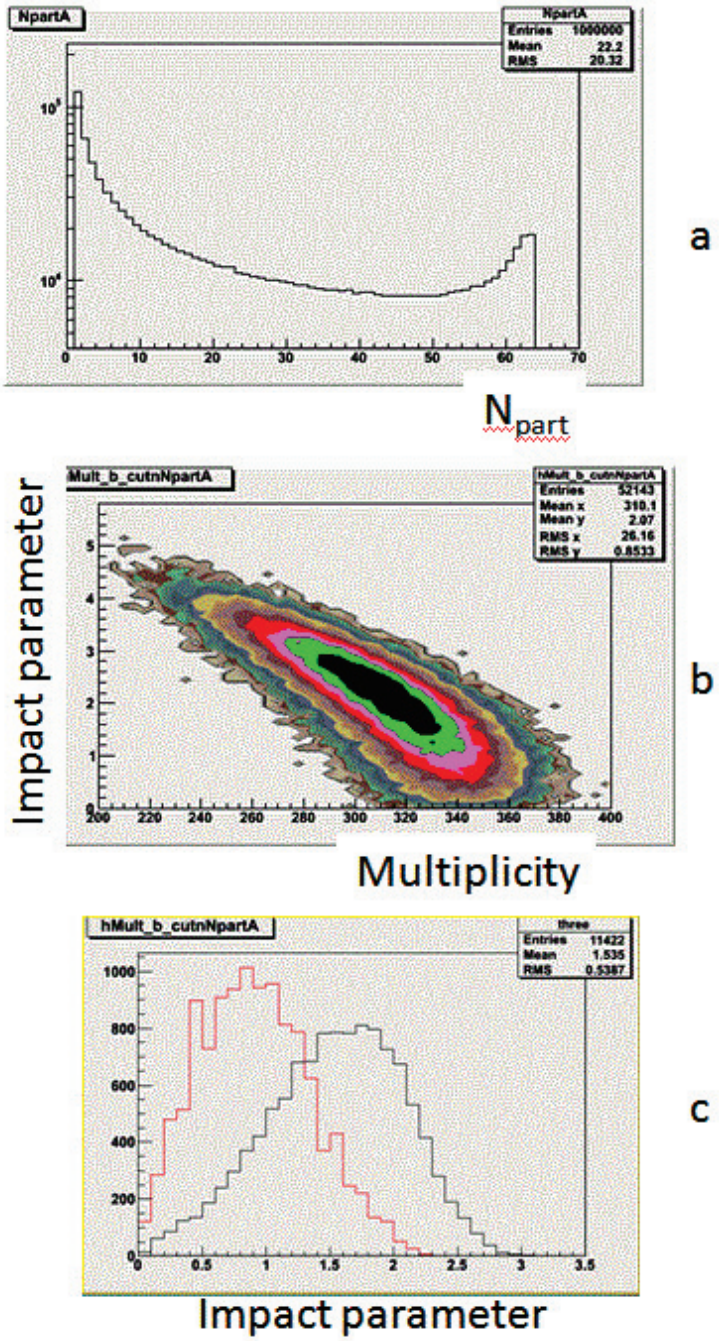

Figure 39: (a) the number of participants in the Cu nucleus in minimum bias Cu+Au collisions. The peak at N_{part} ~62 arises from the case when the Cu nucleus in contained completely in the Au nucleus. (b) The multiplicity vs. impact parameter when the number of participants in the Cu nucleus is greater than 60. (c) The impact parameter when a cut is made for a multiplicity of 360-380 (red) and 320-240 (black). The two distributions are normalized to each other.

5.2.3 U+U collisions

Our fourth priority for Run-13 is to record $0.57nb^{-1}$ of U+U collisions at $\sqrt{s}$ = 193 GeV. We optimistically anticipate being able to demonstrate our understanding of the geometrical selection by offline cuts from the 1.5 week long test run requested in Run-12. Consequently, we request a longer U+U run in Run-13. The motivation and expected statistics were described above.

References

[1] A. Adare, S. Afanasiev, C. Aidala, N. N. Ajitanand, Y. Akiba, et al. Cross section and parity violating spin asymmetries of $W^{\pm}$ boson production in polarized p+p collisions at $\sqrt{s} = 500$ GeV. 2010. arXiv:1009.0505.

[2] A. Adare et al. Energy loss and flow of heavy quarks in Au+Au collisions at $\sqrt{s_{NN}} =$ 200 GeV. *Phys. Rev. Lett.*, 98:172301, 2007. arXiv:nucl-ex/0611018, doi:10.1103/PhysRevLett.98.172301.

[3] A. Adare et al. Gluon-spin contribution to the proton spin from the double-helicity asymmetry in inclusive π^0 production in polarized p+p collisions at $\sqrt{s} = 200$ GeV. *Phys. Rev. Lett.*, 103:012003, 2009. arXiv:0810.0694, doi:10.1103/PhysRevLett.103.012003.

[4] A. Adare et al. Inclusive cross section and double helicity asymmetry for π^0 production in p+p collisions at $\sqrt{s} = 62.4$ GeV. *Phys. Rev. D*, 79:012003, 2009. arXiv:0810.0701, doi:10.1103/PhysRevD.79.012003.

[5] A. Adare et al. Measurement of bottom versus charm as a function of transverse momentum with electron-hadron correlations in p+p collisions at $\sqrt{s} = 200$ GeV. *Phys. Rev. Lett.*, 103:082002, 2009. arXiv:0903.4851, doi:10.1103/PhysRevLett.103.082002.

[6] A. Adare et al. Cold nuclear matter effects on J/ψ yields as a function of rapidity and nuclear geometry in deuteron-gold collisions at $\sqrt{s_{NN}} = 200$ GeV. 2010. arXiv:arXiv:1010.1246.

[7] A. Adare et al. Enhanced production of direct photons in Au+Au collisions at $\sqrt{s_{NN}} = 200$ GeV and implications for the initial temperature. *Phys. Rev. Lett.*, 104:132301, 2010. arXiv:0804.4168, doi:10.1103/PhysRevLett.104.132301.

[8] A. Adare et al. Event Structure and Double Helicity Asymmetry in Jet Production from Polarized p+p Collisions at sqrt(s) = 200 GeV. 2010. arXiv:1009.4921.

[9] A. Adare et al. Heavy quark production in p+p and energy loss and flow of heavy quarks in Au+Au collisions at $\sqrt{s_{NN}} = 200\,\mathrm{GeV}$. 2010. arXiv:1005.1627.

[10] A. Adare et al. Cross section and double helicity asymmetry for eta mesons and their comparison to neutral pion production in p+p collisions at sqrt(s)=200 GeV. *Phys. Rev.*, D83:032001, 2011. arXiv:1009.6224, doi:10.1103/PhysRevD.83.032001.

[11] A. Adare et al. Measurements of higher-order flow harmonics in Au+Au collisions at $\sqrt{s_{NN}} = 200\,\mathrm{GeV}$. 2011. arXiv:1105.3928.

[12] A. Adare et al. Suppression of back-to-back hadron pairs at forward rapidity in d+Au Collisions at $\sqrt{s_{NN}} = 200\,\mathrm{GeV}$. 2011. arXiv:1105.5112.

[13] A. Adil and I. Vitev. Collisional dissociation of heavy mesons in dense QCD matter. *Physics Letters B*, 649(2-3):139–146, 2007. doi:10.1016/j.physletb.2007.03.050.

[14] S. S. Adler et al. Centrality dependence of direct photon production in $\sqrt{S_{NN}} = 200\,\mathrm{GeV}$ Au+Au collisions. *Phys. Rev. Lett.*, 94:232301, 2005. arXiv:nucl-ex/0503003, doi:10.1103/PhysRevLett.94.232301.

[15] M. M. Aggarwal et al. Measurement of the parity-violating longitudinal single-spin asymmetry for $w^{\pm}$ boson production in polarized proton-proton collisions at $\sqrt{s} = 500\ gev$. *Phys. Rev. Lett.*, 106(6):062002, Feb 2011. doi:10.1103/PhysRevLett.106.062002.

[16] B. Alver, B.B. Back, M.D. Baker, M. Ballintijn, D.S. Barton, et al. Importance of correlations and fluctuations on the initial source eccentricity in high-energy nucleus-nucleus collisions. *Phys.Rev.*, C77:014906, 2008. arXiv:0711.3724, doi:10.1103/PhysRevC.77.014906.

[17] B. Alver, M. Baker, C. Loizides, and P. Steinberg. The PHOBOS Glauber Monte Carlo. 2008. arXiv:0805.4411.

[18] Lie-Wen Chen and Che Ming Ko. Anisotropic flow in Cu+Au collisions at $\sqrt{s_{NN}} = 200$ GeV. *Phys.Rev.*, C73:014906, 2006. arXiv:nucl-th/0507067, doi:10.1103/PhysRevC.73.014906.

[19] PHENIX Collaboration. The PHENIX Decadal Plan [online]. 2010. Available from: http://www.phenix.bnl.gov/phenix/WWW/docs/decadal/2010/phenix_decadal10_full_refs.pdf.

[20] RHIC Spin Collaboration. Research Plan for Spin Physics at RHIC [online]. 2005. submitted to U.S. Department of Energy. Available from: http://spin.riken.bnl.gov/rsc/report/masterspin.pdf.

[21] RHIC Spin Collaboration. Research Plan for Spin Physics at RHIC [online]. 2008. submitted to U.S. Department of Energy. Available from: http://spin.riken.bnl.gov/rsc/report/spinplan2008/spinplan08.pdf.

[22] J. Collins, S. Heppelmann, and G. Ladinsky. Measuring transversity densities in singly polarized hadron-hadron and lepton-hadron collisions. *Nucl. Phys.*, B420:565–582, 1994. arXiv:hep-ph/9305309, doi:10.1016/0550-3213(94)90078-7.

[23] D. de Florian, R. Sassot, M. Stratmann, and W. Vogelsang. Global analysis of helicity parton densities and their uncertainties. *Phys. Rev. Lett.*, 101:072001, 2008. arXiv:0804.0422, doi:10.1103/PhysRevLett.101.072001.

[24] M. Djordjevic, M. Gyulassy, R. Vogt, and S. Wicks. Influence of bottom quark jet quenching on single electron tomography of Au+Au. *Phys. Lett.*, B632:81–86, 2006. arXiv:nucl-th/0507019, doi:10.1016/j.physletb.2005.09.087.

[25] Peter Filip, Richard Lednicky, Hiroshi Masui, and Nu Xu. Initial eccentricity in deformed Au-197 + Au-197 and U-238 + U-238 collisions at sNN=200 GeV at the BNL Relativistic Heavy Ion Collider. *Phys.Rev.*, C80:054903, 2009. doi:10.1103/PhysRevC.80.054903.

[26] Heinz:2004ir. Heinz:2004ir. *Heinz:2004ir*, Heinz:2004ir.

[27] X. Ji, J. Qiu, W. Vogelsang, and F. Yuan. A unified picture for single transverse-spin asymmetries in hard processes. *Phys. Rev. Lett.*, 97:082002, 2006. arXiv:hep-ph/0602239, doi:10.1103/PhysRevLett.97.082002.

[28] Kulman:2005ts. Kulman:2005ts. *Kulman:2005ts*, Kulman:2005ts.

[29] Kulman:2006qp. Kulman:2006qp. *Kulman:2006qp*, Kulman:2006qp.

[30] C. Nepali, G. Fai, and D. Keane. Advantage of U+U over Au+Au collisions at constant beam energy. *Phys.Rev.*, C73:034911, 2006. doi:10.1103/PhysRevC.73.034911.

[31] C. Nepali, George I. Fai, and Declan Keane. Selection of special orientations in relativistic collisions of deformed heavy nuclei. *Phys.Rev.*, C76:051902, 2007. arXiv:0709.1497, doi:10.1103/PhysRevC.76.051902,10.1103/PhysRevC.76.069903.

[32] D. Sivers. Hard scattering scaling laws for single spin production asymmetries. *Phys. Rev.*, D43:261–263, 1991. doi:10.1103/PhysRevD.43.261.

[33] H. van Hees et al. private communication.

[34] S. Voloshin. private communication.

[35] S. Wicks, W. Horowitz, M. Djordjevic, and M. Gyulassy. Heavy quark jet quenching with collisional plus radiative energy loss and path length fluctuations. *Nucl. Phys.*, A783:493–496, 2007. arXiv:nucl-th/0701063, doi:10.1016/j.nuclphysa.2006.11.102.

[36] F. Wolfram et al. RHIC Beam Projections [online]. Available from: http://www.rhichome.bnl.gov/RHIC/Runs/RhicProjections.pdf.

[37] R. Yang, J. Peng, and M. Grosse-Perdekamp. Flavor asymmetry of the nucleon sea and W boson production. *Phys. Lett.*, B680:231–234, 2009. arXiv:0905.3783, doi:10.1016/j.physletb.2009.08.070.